POLITECNICO DI MILANO

Department of Informatics, Electronics and Bioengineering

CONTROL DESIGN OF A SURGICAL ROBOTIC PLATFORM FOR ENDOSCOPIC DISSECTION

SARAH ELENA VALDERRAMA HINCAPIÉ

ID: 898053

Supervisors:

Prof. De Momi, Associate Professor in the Electronic Information and Bioengineering Department of Politecnico di Milano

Prof. Menciassi, Full Professor of Biomedical Engineering of Scuola Superiore Sant'Anna, The BioRobotics Institute

The dissertation is submitted for the degree of

Master of Science in Biomedical Engineering

2020

En homenaje a mi familia

Acknowledgements

I would like to express my gratitude to Prof. De Momi for her suggestions and valuable feedback, as well as to Prof. Menciassi, who granted me the opportunity and trusted me to develop this exciting project on robotic surgery.

Secondly, I would like to thank Andrea Mariani for presenting me with the opportunity to work in such a prestige institute as it is the Scuola Superiore Sant'Anna. Additionally, I would like to specially acknowledge Claudio Quaglia, his support and constant guide were precious in the development of the Control Design for a Miniaturized Surgical Robotic Platform project.

Finally, I would like to thank my family. Even in the distance, I felt you right by my side. Without you, any of this would have had any sense.

Sarah Elena Valderrama Hincapié

Abstract

Colorectal cancer accounts with an important morbidity portion occupying the second place worldwide among all the cancer types and the resection of the affected zone is the acknowledged appropriate oncological alternative. Minimally Invasive Surgery (MIS) based on laparoscopy is accepted due to its shorter hospital stay and better aesthetic outcome. However, the complex tilting of the patient due to constraints of the robotic platform along with the risk of metastases at the port site has paved the way towards the development of new robotic surgical tools for endoscopic methods like Endoscopic Submucosal Dissection (ESD) or Endoscopic Mucosal Resection (EMR), which have proven efficiency in the resection of cancerous tissue all while minimizing the already reduced invasiveness presented on MIS.

This study aims to exhibit the control design of a novel miniaturized Robotic Platform for Endoscopic Dissection (RED) of gastrointestinal neoplasms by employing two commercial haptic devices (Omni 3D) as master manipulators, where each one can command one of the two surgical tools, grabbing and cautery arm, of the detachable miniaturized robot. The control strategy is based on a Master/Slave pattern, which is frequently used in Teleoperated systems, and it is composed of three units. The first one, developed in C++, handles the haptic guidance type of the haptic devices and gathers the movement executed by the operator while the second unit processes this information and incorporates security loops to maintain a safe environment to then command the third unit, which is composed by three miniaturized motors that are integrated inside the robot handling the cautery arm, and other three motors kept outside and connected to a cable system, where each of these motors manages one degree of freedom of the grabbing tool. Furthermore, this study proposes a gain scheduling PI algorithm, developed in Matlab and simulated in Simulink, based on fuzzy logic to enhance the adaptation to nonlinearities aiming to improve the PI current loop control in the drivers (EPOS2 24/2) of the Maxon motors.

The proposed control system introduces several haptic functions to block the unused DOFs of the haptic devices while turning the movements of the haptic device executed by the operator into accurate maneuvers by controlling the surgical tools of the robot through the motors. Moreover, the gain scheduling algorithm simulations implementing the PI control models of the motors suggest that this proposed algorithm could surpass the control capacities of the PI one. Experiments supervised and executed by surgeons are formulated as future work. Additionally, it is proposed as future work the introduction of pressure sensors at the tip of the instruments aspiring to introduce feedback in the system through the haptic devices.

Table of Contents

List of Figures

Chapter 1

Introduction

The gastrointestinal interventions are complex due to the anatomical intricated shape and complicated access points the gastrointestinal tract presents. Furthermore, colorectal carcinoma accounts for a high morbidity percentage occupying second place worldwide of all cancer types, and their surgical resection remains the only therapeutic alternative [1], [2].

In the past, the resection of malignant tissue in the gastrointestinal tract was performed via open surgery. However, there were important drawbacks as the risk of infection and morbidity, along with the significant probability of recurrence. The development of technology brought new methods with lower invasiveness, reduced patient recovery time, decline the probability of cancer recurrence, and improvement of the overall outcomes of surgical procedures. One of these methods corresponds to the laparoscopic procedure or in a wider sense to Minimally Invasive Surgery (MIS). This approach is distinguished by reaching the area of interest inside the body via small incisions and employing rigid instruments to operate while observing through an endoscope entered into the body through another small incision. This method improved the outcomes to the patient as the hospital stay was drastically reduced, and the risk of infection was similarly diminished [3]. Even though the outcomes of MIS procedures were indisputable, new concerns arose regarding the dexterity of the surgeons and their feedback perception; furthermore, some studies argued that there was a high probability of local recurrence cancer at the port-site, though, it is potentially associated with poor technical skills [4], [5], [6]. The endoscopic approach is another method proposed in the resection of gastrointestinal cancer to deal with the issues of the open procedures as exploits

the natural orifices to evaluate the internal structures, without breaching their physiological luminal boundaries. Nowadays, this approach is not only accepted for diagnosis but also in the resection of cancerous tumors. Techniques as Endoscopic Mucosal Resection (EMD) or Endoscopic Submucosal Dissection (ESD) are greatly utilized, though, these methods also exhibit reduced maneuverability and limited Degrees Of Freedom (DOF).

Technological frontiers are being pushed even further to propose new methods to strike the drawbacks of conventional surgical procedures and to improve the outcomes of surgery. Robotic systems in the surgical procedures are promising and have been developed throughout the years, bringing increased dexterity along with the enabling simulation to enhance the expertise of surgeons. In the last decade, there was an increase of 572.87% in the research of surgical robotics compared to the former decade [7]. The master-slave architecture is a widely spread configuration when dealing with teleoperated platforms for surgery as proposes to exploit the capacities of the surgeons and transform them into a task developed remotely. The design and considerations for safety, reliability and the human-robot interface are of importance, and this responsibility is conferred to the implementation of an accurate control system. The PID controller has been introduced in the development of teleoperated platforms to regulate the velocity and positioning of the manipulators. However, its performance deteriorates significantly and it can even lead to instability if the motion is fast. Moreover, PID controllers cannot cope with systems that fluctuate throughout time. Gain scheduling PID algorithms based on fuzzy logic and neural network controllers have been proposed to improve the performance of teleoperated systems.

Even though the introduction of robotics platforms for the resection of cancerous tissue in the gastrointestinal tract is encouraging, there are some concerns and challenges that need to be addressed. In the MIS robotic approaches, the splenic flexure mobilization often is unfeasible, because the robotic system may not be able to reach the left upper abdomen, and it may have to be disengaged and reconnected to perform this step of the procedure, which is both a challenge and a shortcoming of the MIS robotic procedures [8]. When covering the challenges of endoscopic methods, the primary one is to compose a proper miniaturized robotic system able to access the body through natural orifices, that maximizes both dexterity and maneuverability of the tools, and to implement the control strategies that allow performing accurate procedures. Much of the current focus is on the development of flexible endoscopic robotic platforms with miniaturized instruments rather than laparoscopic approaches due to their exploitation of natural access points [9], [10].

The Surgical Robotic Platform for Endoscopic Dissection (RED) originated at the Institute of Biorobotics of the Scuola Superiore Sant'Anna is a platform developed to cover these technological calls. The RED system is a novel miniaturized robotic device to be coupled at the tip of a traditional flexible endoscope for the surgical dissection of GI neoplasms, exploiting the flexibility of the endoscope for navigation through the intestine while integrating two-active robotic arms; such combination improves the maneuverability of the entire system, all while reducing the costs associated to the robotic technology.

The present study aims to develop a control strategy to suitably handle the diverse elements of the RED system while ensuring safety and accuracy. As future work, it is proposed to implement the conceived fuzzy algorithm and to incorporate pressure sensors to provide the surgeons with haptic feedback sense that are generally absent or limited reduced in the teleoperated procedures.

1.1 Thesis Objectives

The thesis objective is to develop the control system and to improve the hardware design of a medical robotic device. This device is composed by a six DOFs (Degrees of Freedom) micro-manipulator that is mounted on the head of a traditional endoscope so that it allows to carry out interventions in the field of gastrointestinal surgery under endoscopic visual guidance. The manipulator is endowed with three motors placed inside the robot together with three additional ones that are located in an external box outside the patient: these six motors control the six degrees of freedom. Finally, the surgeon controls the micro-manipulators employing two Phantom Omni haptic devices.

- To examine the current methods used in Minimally Invasive Surgery and to gather information about their advantages and drawbacks.
- To identify the advantages endoscopic approaches have over the MIS procedures.
- To recognize the used architectures in teleoperated systems along with their components.
- To develop adequate functions to control the haptic devices.
- To improve and assemble the parts of the robotic system.

- To construct the system control of a detachable robotic device with prospective use in the resection of cancerous tissue on the gastrointestinal tract.

1.2 Thesis Outline

The current study aims at exposing the advantages endoscopic methods have in comparison with Minimally Invasive Surgery, when dealing with procedures in the gastrointestinal tract. Furthermore, this study exhibits a control strategy implemented on an endoscopic robotic system, composed of two haptic devices and six actuators, with prospective use in surgical procedures for the resection of cancerous tissue on the GI tract.

- INTRODUCTION AND STATE OF THE ART
  - Chapter 1:
    This chapter provides an overview of the present study covering the importance of the development of surgery approaches in the resection of cancerous tissue in the gastrointestinal tract. Furthermore, this chapter highlights the advantages that endoscopic methods have over the MIS ones while illustrating how the inclusion of robotic and teleoperated approaches in MIS and endoscopic methods can provide a solution to their dexterity and accuracy limits.
  - Chapter 2:
    This chapter illustrates the generalities of the gastrointestinal tract covering its anatomical and metabolic functions. In a more detailed approach, the endoscopic and Minimally Invasive methods used in the gastrointestinal interventions are explained, where their advantages, drawbacks, and proper comparison between both of them are covered. Furthermore, it is highlighted the reason why the endoscopic methods are preferred in the gastrointestinal procedures and why most of the scientific developments are focused on them: exploitation of natural orifices and no port-site metastasis.
  - Chapter 3:
    The Telerobotic Surgical Systems chapter provides a detailed explanation regarding the form a teleoperated system is composed, covering the Master/Slave pattern basics, the diverse units usually encountered in this strategy, and provides an overview of the PID controller. Additionally, are illustrated the theoretical basis

of a gain scheduling PI controller aiming to overcome the difficulty in adapting to nonlinearities presented in the PI regulators. Furthermore, this chapter covers the main communication protocols that are used to share information among the diverse electronic devices on Teleoperated system.

- METHODS, MATERIALS, AND RESULTS

  - Chapter 4:
    This chapter illustrates the components and materials conforming the Robotic Endoscopic Device (RED) for tissue resection designed at the Institute of Biorobotics of The Scuola Superiore Santa'Anna, which is the platform the present study is aiming to improve and to design its control strategy. Furthermore, it is given an overview of the mechanical system, design, and functioning of this teleoperated robotic platform.
  - Chapter 5:
    The present chapter covers both methods and results, where the first part illustrates the control design workflow and utilized commanding programs, such as LabVIEW and the DLL library created in C++. Additionally, it illustrates the geometrical and algebraic approaches used to create haptic guidance types. This chapter also depicts the derivations of the Gain scheduling PI controller along with the corresponding simulations of the motor velocity loop model, conceived on Simulink. Finally, it is given a description, in a pseudo algorithm form, of the main control system developed in the programming language LabVIEW.

- DISCUSSION, CONCLUSIONS, AND FUTURE WORK

  - Chapter 6:
    The concluding chapter of the present study corresponds to the discussions and conclusions found in its development. Initially, it is covered how the approach followed to design the control system of RED platform resulted in a sufficiently accurate and secure method to perform independent maneuvers of the surgical tools. Furthermore, it is highlighted how haptic guidance in the master devices can provide a more controlled and self-explanatory environment to the operator. It is also illustrated that even though PID controllers have been widely employed and are trusted control mechanisms, it lacks nonlinearities regulation. The introduction of adaptable gain scheduling could improve the performance of these controllers.

Chapter 2

Gastrointestinal Surgery

The gastrointestinal tract procedures have earned special attention in the health system as the colorectal carcinoma is a frequently encountered tumor. Only in the United States it is estimated to diagnose 148810 new cases; additionally, it accounts with a high morbidity percentage occupying the second place worldwide among the cancer types [2]. An improved understanding of the growth of early gastric carcinoma and lymph-node spread has meant that resection of the affected zone has become an oncological appropriate surgical option [11].

The surgical procedures for the dissecting of malignant tissue in the gastrointestinal tract comprehend extra-luminal methods, intra-luminal techniques, and the conventional but limited open procedures. The intra-luminal or endoscopic procedures are characterized by entering the body through natural orifices while the extra-luminal or laparoscopic ones need small incisions to access the area of interest inside the body, both of them, compared to open surgery bring improvements in safety, accuracy and shorter hospital stay along with better oncologic outcomes [12], [8]. However, in terms of dexterity, learning curve, and cost-effectiveness improvements need to be developed.

The gastrointestinal interventions are especially challenging due to the anatomical complexity and complicated access points, drawing the attention of engineers as the improvement of safety, accuracy, and dexterity on endoscopic procedures and Minimally Invasive Surgery are key points for their proper adoption and further benefits to the surgeons and patients. The usage of the laparoscopic technique has largely replaced open colorectal surgery [11], but much of the current focus is on the development of flexible endoscopy due to its exploitation

of natural access points [9]. Moreover, concerns about port-site metastases have limited the application of minimally invasive surgery for intra-abdominal malignancies but it is believed that poor surgical technique is a causative factor in port-site metastases [6]. The implementation of robotics platforms is a potential key factor to strike these concerns as the increased dexterity brought by these systems along with the enabling simulation to increase the expertise of surgeons is promising, yet, the oncologic outcome of robot-assisted rectal resection is still a subject for future investigation [8].

In this chapter, the prevailing trends on robotic surgery employed in the gastrointestinal tract along with the advantages and drawbacks these diverse approaches can bring are explained. In segment 2.1, the anatomical properties of the gastrointestinal tract are established while section 2.2 includes the endoscopic features and its methods. Additionally, part 2.3 comprises the generalities and constrains of Minimally Invasive Surgery. Finally, section 2.4 illustrates the robotics technologies to face the gastrointestinal surgery challenges, covering their advantages and possible complications.

2.1 Gastrointestinal Tract

The gastrointestinal tract (GIT) is a muscular tube with a largeness of around $6m$ with varying diameters which oversees digestion and absorption of nutrients coming from the ingested food. The GI tract is composed by four principal anatomical areas (Fig. 2.1); the esophagus, stomach, the small and the large intestine [13]. The most relevant zone of the GI tract for the present study corresponds to the lower one (small and large intestine) as the aim is to develop an endoscopic detachable robotic system for the dissection of potentially cancerous tissue in this area.

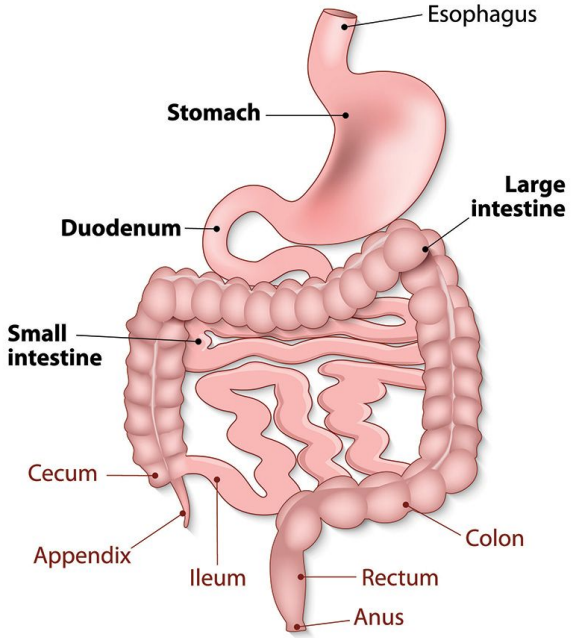

Fig. 2.1 Gastrointestinal tract physiology

The small intestine, located at the base of the stomach, is distinguished by having a lengthiness of around $5m$ and a diameter of $3cm$; it is also recognized by being responsible for merging the nutrients with digestive juices, mostly made by the mucosal cells [14].

The large intestine, commonly known as the colon, is placed right after the small one and possesses a $1.5m$ length where its diameter decreases from $7cm$ to $4cm$ [15]. The main function of the large intestine is the re-absorption of water [16].

2.2 Endoscopy

The endoscope was developed in 1960 and it allowed rapid technology development in the surgical area. It is a highly flexible device that combines fiber-optic technology and charge-coupled devices to facilitate illumination and visualization to perceive the status of a specific area inside the body, thus, enabling to inspect, diagnose and clinically evaluate the zone through a computer monitor [3], [17].

The endoscopic or intraluminal procedures are performed to evaluate structures that are exposed to the external environment at one of their extremities all without breaching their

physiological luminal boundaries, *i.e.* avoiding incisions [3]. The gastrointestinal tract is usually grappled with endoscopic interventions precisely due to the possibility of accessing it through the anus and also considering the benefits that this technique provides compared to open surgery *e.g.* reduced recovery time, lower risk of infection, and diminished total morbidity [18]. However, the GI tube-like shape throughout its largeness along with the intricated shape, non-uniform diameter, highly flexibility and fragility represents a challenge and imposes more complex interventions that require more dexterous surgeons [13]. Fig. 2.2 shows a colonoscopy in the large intestine depicting the demanding tasks faced during endoscopic interventions due to the intricate silhouette of the intestine.

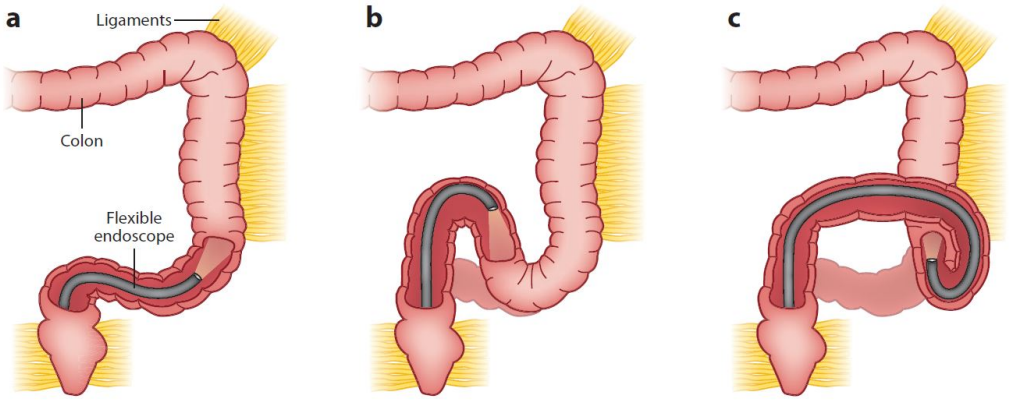

Fig. 2.2 Endoscope flexibility problem in colonoscopy. The desired situation is depicted in a), the in practice is depicted in b) while the painful situation for the patient in c) [15].

At first, the endoscopy employed in the gastrointestinal tract was aiming at evaluating and diagnosing its structure, though, in recent years, diverse tools have been developed to expand its applications, and we can find among them the assessment of the mucosa, resection of polyps, management of bleeding, and gathering of tissue samples. [17]. Due to these advantageous possibilities, the intraluminal endoscopic treatment methods are increasingly replacing open surgical resection or even laparoscopic technique [19]. Among these techniques we can encounter: Endoscopic Mucosal Resection (EMR), Endoscopic Submucosal Dissection (ESD), Transanal Endoscopic Microsurgery (TEM) and Transanal Natural Orifice Transluminal Endoscopic Surgery (NOTES). In the present study, TEM and especially ESD are going to be the subjects of attention.

2.2.1 Endoscopic Mucosal Resection

Gastrointestinal Endoscopic Mucosal Resection (EMR) is a procedure to remove cancerous tissue from the digestive tract usually when the area to be extracted is larger than 10*mm*. This technique is based on endoscopy and makes use of a snare to capture the targeted tissue. Local injection of a solution of hypertonic saline-epinephrine (ERHSE) is used to elevate the lesion, then an electrosurgical current is employed to extract the damaged zone [20]. The abstraction process performed by this type of procedures is depicted in Fig. 2.3.

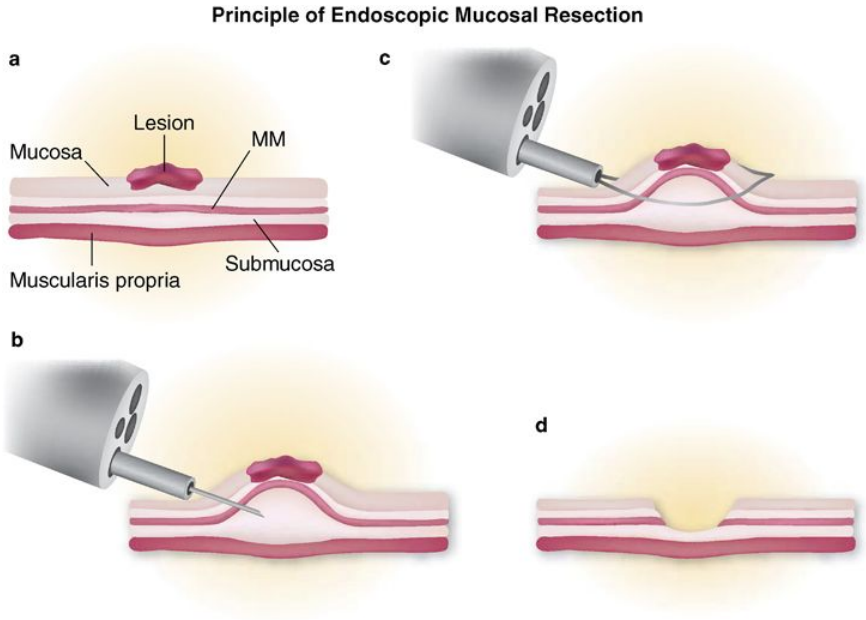

Fig. 2.3 Endoscopic Mucosal Resection procedure [21].

Even though EMR is a procedure that has been widely executed in the past years in the gastrointestinal tract [22], it accounts with a drawback consisting on the need of removing the tissue in a piecemeal way when the lesion is larger than 15*mm*, provoking an increased probability of internal bleeding and tumor recurrence.

2.2.2 Endoscopic Submucosal Dissection

The Endoscopic Submucosal Dissection (ESD) is a technique used for the complete resection of early-stage lesions in the gastrointestinal tract and is based on the principles of the EMR, although it is considered safer and of superior efficacy [22]. The ESD is a

technique that utilizes flexible endoscopy permitting bloc resection of superficial lesions on the digestive tract [23].

This technique consists of three different steps. The first one is comparable to the initial step in EMR and corresponds to the injection of a substance into the tissue while the two following actions differ from the EMR in the sense that instead of grabbing the complete afflicted tissue and using a cautery system, the area is cut permitting the extraction of a more specific zone and to remove tissue under the lesion [24]. Fig. 2.4 depicts the stages of the intervention. The last step is the key point and main advantage of the ESD as dissecting tissue under the lesion diminishes the tumor recurrence. However, being the ESD a more complex procedure compared to EMR, its augmented dexterity and adequate personal training are needed to evade complications associated with perforations and prolonged procedure time [22].

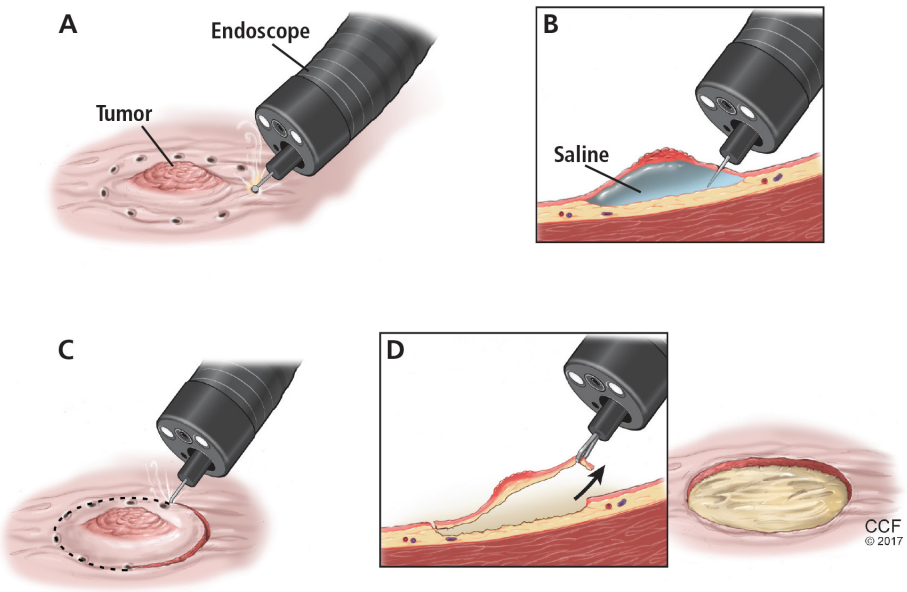

Fig. 2.4 Endoscopic Submucosal Dissection procedure [25].

The reduction of tumor recurrence along with the greater accuracy have made the ESD a subject of interest in the engineering and medical fields [26]. In the past 10 years, several assistive devices have been elaborated to reduce the maneuverability complexity of this technique along with expanded tools and employment of valuable surgical equipment to increase its adoption, as it is the EVIS EXERA III® (See Fig. 2.5).

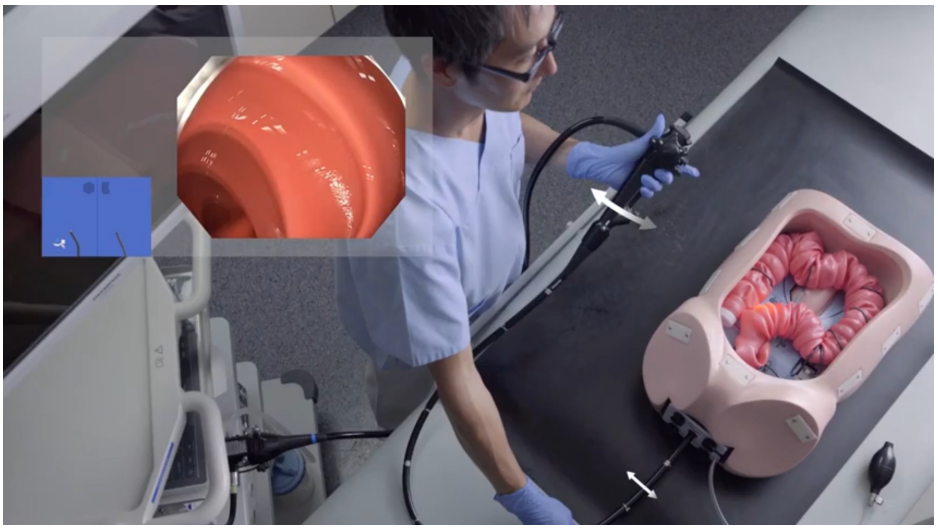

Fig. 2.5 EVIS EXERA III® by Olympus, Inc. The wider picture depicts the positioning of the tools and surgeon while executing an ESD procedure while the shorter one illustrates the reduced workspace inside the GI tract and the tip deviation of the flexible endoscope.

EVIS EXERA III® is one of the most recent and advanced systems used in ESD procedures. This system allows the surgeon to have further control at the tip by implementing mechanical control, allowing left to right motion. However, the movements at the tip of the tool are not subtle, and by not having haptic guidance to execute the actions, the surgeon can get disoriented and execute forbidden moves.

2.2.3 Transanal Endoscopic Microsurgery

The Transanal Endoscopic Microsurgery (TEM), differently from the ESD and EMR, is a technique which is not based on a flexible endoscope and free moving tool, but the entire system is fixed to the operating table and it is composed by a set of endoscopic surgical instruments along with an assisted vision, usually stereoscopic. Furthermore, the instrument possesses a higher diameter than the regular endoscopes used in ESD and EMR techniques, summing the fact that TEM needs sphincter dilation to keep the field of vision and access, this being achieved either by employing the injection of a dilatory substance to the patient or by continuous insufflation of the rectus [27].

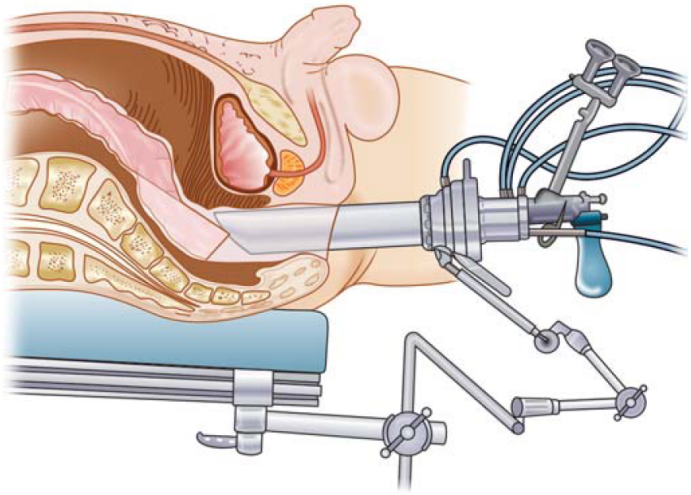

Fig. 2.6 Transanal Endoscopic Microsurgery procedure [28].

Minimally invasive procedures used in the GI tract can be employed to treat rectal adenomas or intramucosal cancer. The TEM is distinguished by having up to four surgical instruments that can reach further into the rectum allowing the resection of tumors located in the range of 4-18cm from the anal verge, encompassing the extraction of rectal tumors in the low, middle and upper part. The diameter of the rectoscope used in TEM is around 4cm and its largeness varies from 12-20cm, depending on the targeted point position.

2.3 Minimally Invasive Procedures

Improvements in surgery have been focused on minimizing the invasiveness, enhancing the accuracy and reducing the recovery time of surgical procedures. Laparoscopy has been by far the most frequent and standardized surgical technique as its proven safety and efficacy have been demonstrated in several abdominal surgeries [19], [9]. Laparoscopic procedures, titled as extra-luminal interventions, consist of accessing the body via small incisions made in the abdominal wall, called port-sites. The rigid instruments are anchored to these port sites and are placed inside the patient aiming to approach the surgical target. It is particularly important to note that to improve the angle of vision and the workspace in the laparoscopic procedures, the insufflation of gas is required [3].

The incursion on laparoscopy aided the development of diverse methods with applications that varies from neurosurgery to arthroscopy. Minimally Invasive Surgery (MIS)

comprises all of them and its methods are characterized by accessing the body through small incisions enabling to assess areas that were before difficult to achieve or imposed high-risk interventions, all while diminishing the hospital stays and improving cosmetic results when comparing these type of methods with the conventional open surgery [8]. The gastrointestinal tract procedures are specially benefited by Minimally Invasive Surgery, due to the prior mentioned advantages and summing the fact that conventional open procedures convey probable higher local cancer recurrence [8], yet, MIS techniques are technically demanding, and the experience and skills of the surgeons are fundamental [11], [18]. Moreover, concerns about increment of port-site metastases have limited the application of minimally invasive surgery for intra-abdominal malignancies [6], though, this drawback is comparable to that of open surgery [8]. Studies have shown that this increment of local recurrence on the port-site is potentially associated with poor technical skills and it is precisely one of the points that technological advance should address [4].

The development of Minimally Invasive Surgery is still at the very beginning of its potential profits for the health care system, surgeons, and patients, being that the reason why technological efforts have been focused on it. Throughout the years, advancements on robotics and teleoperated platforms, along with their application in diverse areas, such as MIS, have made possible with every passing day the reduction of the MIS drawbacks and their introduction into the healthcare system have started to become more feasible [3].

2.4 Teleoperated Robotic Surgery

The introduction of robotics systems into the medical field aims to exploit and complement human capabilities since its prospective advantages are to upsurge the operational efficiency, to increment the dexterity, and improve the observational capabilities of the surgeons [29]. The robotics systems used in surgery can be thought of as smart surgical tools able to improve the efficacy, safety, and reduce the burgeon of the surgeons while meaning to the patients possible lower morbidity and faster recovery times. Furthermore, the integration of diverse sensors and augmented field of vision along with the effortless sterilization process can escalate the advantages that these types of systems have compared to the traditional surgery [30].

We can distinguish two types of robotics platforms in surgery: surgeons' extenders and the auxiliary surgical supports. The former mentioned, consists of a system directly

commanded by the surgeon and among its advantages, we can find a lessening of hand tremor, augmented dexterity, and the introduction of a smaller end-effector (EE), *i.e* narrower tools compared to the size of human's hand. As for the auxiliary surgical supports, they intend to work side-by-side with the surgeons and perform tasks that increase the surgeon's freedom or can decrease their burden by performing extenuating tasks as holding the endoscope or keeping the anatomic target in the field of view [31].

Robotics surgery offers technological solutions to current challenges of minimal access surgery, both intra-luminal and extra-luminal, in diverse specialties of medicine. In the past decade, the most researched area on robotics surgery was urology, followed by gastrointestinal procedures where robot-assisted rectal surgery has received special interest [8], [32]. Robotics procedures are particularly appropriate for adoption in the gastrointestinal tract by their attribute to achieve high operational accuracy even in concealed regions. Moreover, he mazy shape of the GI tract introduces a clinical challenge and the insertion of robotics platforms can potentially alleviate this demanding task.

When talking about techniques used in the gastrointestinal tract we can demarcate extra-luminal and intra-luminal methods. The first one, usually titled as MIS, accesses the body through a small incision called trocar; by implementing robotics platforms we can solve diverse issues that the conventional laparoscopic surgery possesses as the fulcrum effect or the hand tremor. As per the intra-luminal methods, the exploitation of natural orifices to access the area of interest offers a reduction of the already diminished invasiveness of the laparoscopic procedures and by implementing robotics platforms it is possible to enhance the maneuverability of the surgeon and improve dissection capabilities compared to conventional techniques like ESD or TEM. Much of the current focus is on the development of flexible endoscopic robotic platforms with miniaturized instruments rather than laparoscopic approaches due to their exploitation of natural access points [9], [10].

In general, we can see the robotics systems used in the resection of cancerous tissue on the gastrointestinal tract as platforms able to outperform conventional methods and improve the disease-free survival likelihood of the patients [4]. Furthermore, the introduction of robotics platforms promises to improve the dexterity of the surgeons thus enhancing their technical performance which has been demonstrated to be a key point in reducing the tumor recurrence and alleviate the port-site metastases associated with Minimally Invasive Surgery.

2.4.1 Minimally Invasive Teleoperated Robotic Procedures

Conventional MIS comprises advantages as the already mentioned reduced hospital stay and better cosmetic results; nevetherless, these type of procedures come with drawbacks compared to open surgery as it is the loss of the stereoscopic depth perception, the not directly control of the visual space by the surgeon, since the endoscope is controlled by an assistant, and the high fatigue of the personnel. Additionally, the rigid instruments and the fulcrum effect at the port-site in the laparoscopic procedures reduce the dexterity capabilities of the surgeons along with the sensory feedback. Hence, in conventional laparoscopy, tasks like ligation and suturing are much more complex. Moreover, advanced laparoscopic surgery has a technically more demanding learning curve if compared with open surgery, being this especially applicable to colorectal surgery as its narrowed operative field, preservation of the hypogastric plexus, as well as obtainment of clear resection margins, are of paramount importance [33], [8]. Robotic technology was introduced to alleviate some of these constraints [9].

In 1997, Intuitive Surgical Inc came out with a robot prototype with prospective use in Minimally Invasive Surgery, titled the da Vinci, which was a master-slave manipulator with three arms, one for the endoscopic camera and the other two arms aiming to hold the operating instruments. Since its introduction into the market, several breaking technology and new features have been developed to be incorporated into the da Vinci Surgical System and to improve its performance such as articulating end-effectors, tremor abolition, and increased degrees of freedom that significantly augmented surgical dexterity in MIS [9]. The da Vinci Surgical System has proved to be a breakthrough technology and stood the test of time since its inception [33].

The specialties where the introduction of the da Vinci Surgical System (Fig. 2.7) has improved their accuracy and outcomes are vast. One area of particular interest is the gastrointestinal tract, as its complex S-shape and anatomical position impose demanding tasks to both open procedures and conventional laparoscopy. The da Vinci Surgical System enables a fine dissection in the narrow pelvis, improving accuracy and reducing the complications. These technical advantages are intended to achieve better oncologic and functional outcomes after rectal cancer surgery [4].

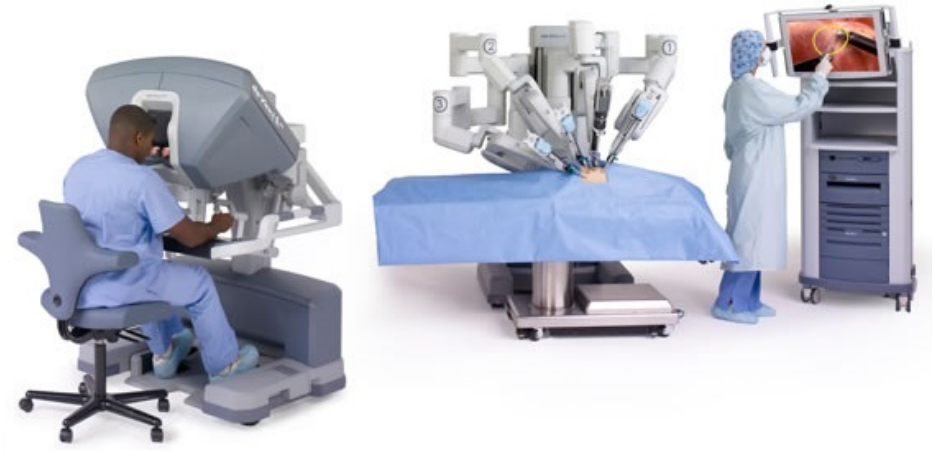

Fig. 2.7 The da Vinci Surgical System®, Intuitive, Inc.

There are, however, several shortcomings associated with robotic rectal resections in MIS. First, the robotic system may not be capable to reach the left upper abdomen, and it may have to be disengaged and reconnected to perform the procedure properly. Second, the tilting of the patient is constrained by the robotic system, thus, bulking of the small intestine may prove problematic during the surgery. Third, an improved view of the vascular and nerve structures of the pelvis is still needed to be developed and implemented in MIS robotic systems [8]. Last but not least, the already mentioned port-site metastases creates some reservations concerning the adoption of MIS procedures in gastrointestinal tumor resection [6]. Despite the aforementioned drawbacks, robotic MIS is encouraging and future developments are aiming to solve the inconveniences here explained.

2.4.2 Teleoperated Robotic Endoscopy

The traditional endoscopy exploits the natural orifices of the human body as points of access to achieve specific targets in the gastrointestinal tract. However, the diverse techniques available hold weaknesses due to the limited quantity of accessible tools, the high work load imposed to the surgeons and the reduced maneuverability due to the loss of Degrees of Freedom (DOFs) due to confined space [34]. Manual control of existing endoscopic technology is likewise not suitable for navigation through the three-dimensional and complex abdominal cavity that requires several maneuvers and fine control of the endoscope tip [9]. The robotic endoscopic systems have been precisely developed aiming to cover these needs and to improve already implemented and trusted methods, as EMR or ESD, by enhancing

their accuracy, effectiveness, safety, reliability to enhance the interventional capabilities of endoscopists, and by increasing the available tools and expanding the degrees of freedom to heighten the dexterity of the surgeons [35].

Current efforts in the development of flexible robotics endoscopy are focused on the expansion of tools able to be maneuvered in very small and geometrically complex spaces along with the introduction of new actuation technology, where this type of robotic endoscopy is titled Driven instrumentation [36]. Typical instruments have 3 degrees of freedom (DOFs) and consist of insertion, rotation, and grasping. The reduction of costs that are associated with the introduction of robotic platforms is a key point in the implementation of robotics endoscopy technology. As a consequence, there is a high trend that points towards the design of robotic devices that incorporate a common central core of technology, to which other sub-devices can be attached offering the possibility of systems with exchangeable tools [18], [9].

The Driven instrumentation robotics systems utilize cable actuation and usually, the driven instrumentation platforms are mounted externally to a conventional endoscope [36], as depicted in Fig. 2.8.

Fig. 2.8 Flexible robotic endoscopy system (Flex® Robotic System developed by Medrobotics, Inc).

The MASTER system is the first robotic-assisted endoscope, titled EndoMaster, able to remove gastrointestinal tumors. However, this prototype possesses a bulky control unit.

Another introduced system was the ISIS-Scope/STRAS [36], developed in the 2013 in Europe, and this robotic platform has the advantage of enabling the passage of instruments, though, improvements regarding its size are needed. In 2012, a system developed in Belgium was designed to utilize magnetic sensors that enabled the localization of the end-effector by placing these sensors at its tip, but the implementation of these kinds of sensors resulted in a bulky system. The EndoSamurai, a further platform, made use of a conventional endoscope, an overtube, and two flexible arms [36]. In 2016, the Robotic Platform for Endoscopic Dissection (RED) was developed at the Scuola Superiore Sant'Anna, which has a characteristic distinction from the other endoscopic robotic systems already introduced in the market: offers the possibility of effortlessly attach and detach a miniaturized robotic device with two tools and 6 total degrees of freedom, able to exploit the endoscope capabilities for navigation through the intestine [37]. In Chapter 4, this system will be explained in detail.

Chapter 3

Telerobotic Surgical Systems

Telerobotics surgery proposes to exploit the surgeons' capacities and transform them into a developed task delivered in the distance. There are telerobotic surgery systems that can operate within miles. The design and considerations for safety, reliability and the human-robot interface are of fundamental importance, and a trusted method to command these systems is the master-slave arrangement.

A telerobotic operation system with a master-slave layout consists of several subsystems. One of the parts is the master manipulator and is responsible for capturing the information coming from the human operator, allowing to command the slave arm. Another subsystem is the slave manipulator, which is in charge of executing the operation using end-effectors that mimic the movement of the master manipulator. The local control subsystem deals with the regulation of the schema to provide precise and fine motion, both to the master and the slave manipulator. Lastly, the information channel is the unit in charge of leading the way information is transmitted while ensuring that all components on the system, as actuators, drivers or haptic devices, are properly addressing the data.

The design of accurate control systems with improved safety and the ability to provide feedback data to the operator has been widely researched. Since the very beginning of teleoperation, PID controllers have been applied to systems involving slow movement. However, its performance deteriorates significantly and even lead to instability if the motion is fast. Moreover, PID controllers cannot cope with systems that fluctuate through time [38].

In this branch, are covered the main technologies and components that constitute telerobotic operation. Segment 3.1 presents a master device highly used in the academic field while section 3.2 includes the characteristics of the actuator in the slave manipulators. Additionally, part 3.3 comprises the generalities and constraints of the PID controller along with an updated gain scheduling version of it. Finally, section 3.4 illustrates the communication interfaces to deal with the long-distance challenge between the diverse components in telerobotic surgery systems.

3.1 Master Manipulator

A master manipulator is controlled directly by the human operator, then, this input coming from the operator is transmitted to the slave arm to implement the given task, meaning that the slave arm duplicates the motion of the master manipulator. There are different master devices, here the PHANToM Omni haptic device is going to be addressed.

The PHANToM haptic input system (See Fig. 3.1) is an electromechanical device with kinesthetic feedback. This device has been implemented in recent years in medical applications and teleoperation and consists of 6 DOFs where all its joints are rotational but only the first three, which proportionate the translational movements, are actuated. The remaining three joints correspond to the rotational movements of the gimbal [39], [40].

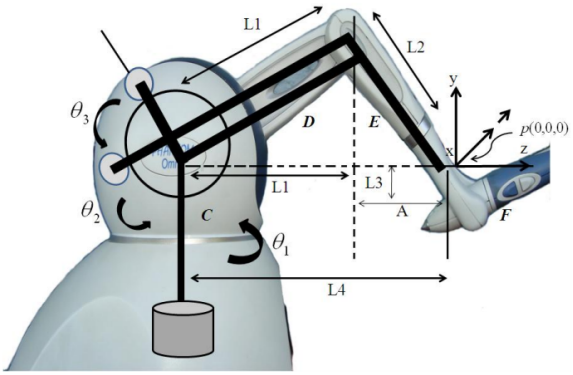

Fig. 3.1 PHANToM kinematics [39].

The forward kinematics of a manipulator concedes to relate the cartesian coordinates and the joints position of the device. Fig. 3.1 represents the haptic device and its corresponding

joints and characteristics while Equations 3.1 provides the synthesis of the computations to find the cartesian coordinate trajectory [39].

$$
\begin{aligned}
x &= \sin\theta_1 (L_2 \sin\theta_3 + L_1 \cos\theta_2) \\
y &= -L_2 \cos\theta_3 + L_1 \sin\theta_2 + L_3 \\
z &= L_2 \cos\theta_1 sin\theta_3 + L_1 \cos\theta_1 \cos\theta_2 - L_4
\end{aligned}
\tag{3.1}
$$

The three passive rotational axes of the gimbal give the pitch, roll, and yaw axis of the rotation movement done on the end-effector.

3.2 Slave Manipulator

The slave manipulators move following the motion of the master manipulator produced by the operator and they are articulated mechanical devices composed by several joints that are actuated by motors, thus, the commanded part by the master is, in reality, the position, torque, and velocity of the motors. However, motors tend to include high weights and occupy important space in the structure of the manipulators [41]. The Brushless DC motors (BLDC) were precisely introduced in slave manipulators to solve the necessity of incorporate actuators with a reduced size while increasing the ratio of the delivered torque [42].

The BLDC motors do not use brushes for commutation as the standard DC brushed motors; instead, they are electronically commutated, which suggests that the stator windings should be energized in a sequence. It is important to know the rotor position to understand which winding will be stimulated following the energizing sequence. The rotor position is usually sensed by using three Hall effect sensors embedded into the stator, where depending on the combination of these three signals it is possible to determine the position [42]. However, it is not accurate and regularly, to improve the calculation of the position encoders are incorporated into the system.

3.3 Control System

A control scheme is designed specifically to regulate a system, aiming to achieve the desired output values while ensuring an aspired level of performance. Every system we come in contact with is developed by sophisticated control methods and examples vary from temperature regulation in air-conditioners to more sophisticated systems such as the family car [43].

Control system design in practice requires cyclic effort in which one iterates between modeling, design, simulation, testing, and implementation. To carry out control successfully it is unavoidable to combine multiple disciplines including modeling, electronics, communications, computing, and interfacing the multitude of different components [43].

The science of automatic control offers a wide extent of choices for control schemes, covering the conventional PID schemes to adaptative controls like neural networks. In the present research, the PID and fuzzy controls are going to be the center of attention.

3.3.1 Proportional, Integrative and Derivative Controller

The proportional-integral-derivative (PID) control offers simple, clear functionality, applicability and yet efficient solution to many real-world control problems. The PID controller minimizes the changing error in the inputs of the system while covering treatment to both transient and steady-state responses [44].

PID working principle is that error value ($e(t)$) is computed from the processed measured value, ($y(t)$) and the desired reference point ($r(t)$). The proportional gain (K_P) provides an overall control action to the error signal, while the integral term (K_I) reduces the steady-state errors through low-frequency compensation by an integrator. The derivative term (K_D) improves transient response through high-frequency compensation by a differentiator. Equation 3.2 presents the mathematical derivation of a conventional PID controller.

$$G(s) = K_P + K_I \frac{1}{s} + K_D s \tag{3.2}$$

When analyzing the entire system in a closed loop (See Fig.. 3.2) we have

$$e(t) = r(t) - y(t) \tag{3.3}$$
$$u(t) = K_P e(t) + K_I \int_0^t e(\tau)d\tau - K_D \frac{d}{dt} y(t)$$

Composing and tuning a PID controller resembles to be conceptually intuitive, but can be hard in practice, especially if multiple objectives such as short transient and high stability are to be achieved. Efforts are profoundly focused on finding disruptive technology able to assist engineers to achieve the best overall performance. Furthermore, it is worth to mention that PID controllers are characterized for having fixed gains; consequently, they are not entirely accurate when dealing with nonlinear systems.

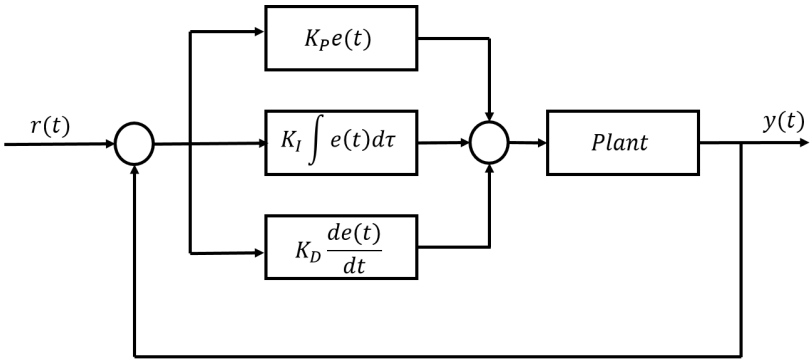

Fig. 3.2 PID controller on close loop.

Manufacturers have tried to introduce into their hardware PID control modules with tuning on-demand or adaptive tuning or both, aiming at diminishing the limited capacities of PID schemes to regulate accurately non-linear systems.

Tuning on demand is characterized by having the need to be re-tuned periodically and whenever changes occur in the process dynamics, while the adaptive tuner possesses a range of changes that can be covered and is rather limited, the model is still needed for determining initial PID settings. Although, once the controller is properly configured it can constantly monitor the process and adjust the parameters [44].

3.3.2 Fuzzy Algorithm Control

Physical changes in the machinery due to usage or even temperature variations can make a system change its dynamics, thus almost all processes are nonlinear. A nonlinear process is a difficult task to face when designing the control system, and traditional strategies as PID controllers might not be sufficient to achieve the desired performance. However, if the control strategy can be expressed qualitatively, a fuzzy controller can be of help as it emulates a heuristic rule-of-thumb strategy.

The fuzzy logic is a method of rule-based decision making used for expert systems and process control. The fuzzy logic controller employs the control rules of conditional linguistic statements on the relationship of the system variables and emulates the behavior of a human operator to deal with the uncertainty of the processes [45]. This controller, as shown in Fig. 3.3, consists of main four parts: fuzzyfication, rule base, inference engine, and defuzzification.

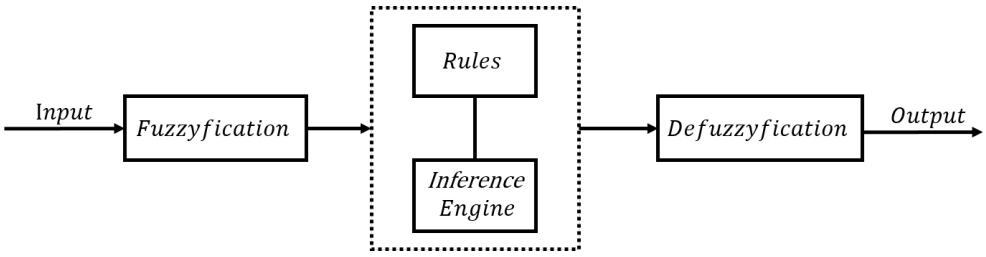

Fig. 3.3 Fuzzy logic [46].

Fuzzification is the process of associating numerical input values with the linguistic terms of the corresponding input linguistic variables, performed by the membership functions. A membership function (MF), describes by numerical functions the degree of membership of linguistic variables within their semantic terms. Later, the fuzzy controller utilizes the rules to determine the resulting linguistic terms of the output, which are semantic variables. Lastly, the defuzzification is in charge of transforming the degrees of membership of the linguistic output into numerical values.

Even though the fuzzy logic is profoundly relatable to the human one, its difficulty lies in suitably designing the membership functions and its rules.

3.3.3 Fuzzy Gain Scheduling of PI Controllers

The traditional proportional-integral controller (PI) is broadly used in control systems due to its simple structure and convenient performance; however, its parameters are initially calculated according to the current parameters, though in practice, these change inevitably throughout time. The combination of the fuzzy logic and PI controller, in which the PI parameters can be adjusted online by an adaptive mechanism based on a fuzzy inference system, promises to be the next level in control system designs. Fig. 3.4 depicts the scheme of this type of controller.

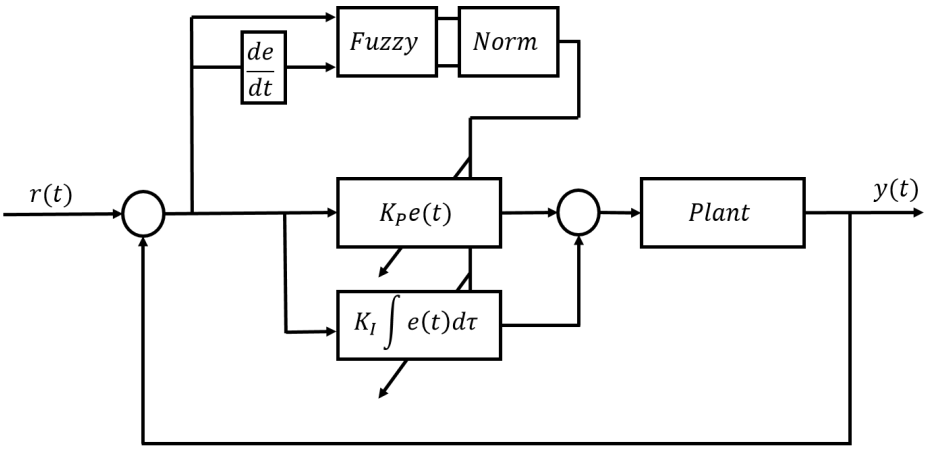

Fig. 3.4 Fuzzy PI gain scheduling.

A normalization method of the inputs is required to keep the transformation of this data proportionally and define the ranges within which the gains will be adjusted automatically to achieve the control target, Equation 3.4 denotes the rules to normalize the data. In the fuzzy gain scheduling control scheme (Fig. 3.4), the normalization is expressed on the block called *Norm* [47].

$$K'_P = \frac{K_P - K_{Pmin}}{K_{Pmax} - K_{Pmin}} \qquad (3.4)$$
$$K'_I = \frac{K_I - K_{Imin}}{K_{Imax} - K_I Pmin}$$

Then, the updated PI parameters are

$$K_P = K'_P(K_{Pmax} - K_{Pmin}) + K_{Pmin} \tag{3.5}$$
$$K_I = K'_I(K_{Imax} - K_{Imin}) + K_{Imin}$$

Lastly, the steps that need to be followed to find the proper range of each of the gains in the fuzzy logic are:

1. Let $K_{Pmin} = K_{Amax}$ and $K_{Imin} = K_{Imax}$ be the lower and upper bounds of the calculated gains (output) $K_{P'}$ and $K_{I'}$, respectively [48].

$$K_{P'} : [K_{Pmin}, K_{Pmax}]; \tag{3.6}$$
$$K_{I'} : [K_{Imin}, K_{Imax}];$$

2. Adjust the bounds and observe the control result. First, change one bound and if the control result is improved, keep on changing in the same direction. Otherwise, restore the changed bound and move on to another bound. This step should be exercised repeatedly until the satisfying result [48].

Lastly, apply the gain scheduling PI controller which uses the fuzzy logic by following Equation 3.5.

3.4 Information Exchange Protocols

The information exchange occurs in a group of devices that need to manage the transmission of information between them to achieve a given task, an example of this type of communication group is a master-slave system. There are different types of communication groups and their classification depends on the way the association between the devices is made. The peer-to-peer model is restricted to a unidirectional trade of information between two devices, while the multicast one allows the introduction of several receivers and one sender, thus, keeping the unidirectional characteristic of the peer-to-peer organization. The concast type, contrary to the multicast, grants to incorporate various senders that transfer their

information to one receiver, though, the exchange is also unidirectional. Finally, the multipeer interchange comprises all the aforementioned types as allows to fuse several senders and receivers all while having a bidirectional exchange of information, meaning that every group member is a potential sender or receiver [49].

The communication protocol was born precisely due to the complexity to manage the exchange of information and aims at studying a method to control the traffic, and in that way, keeping the transference of information between senders and receivers as intact as possible. The communication protocols consist of defining rules to enable proper message interchange, to promote secure and authenticated communication between devices [49]. There are several protocols and the employment of each of them depends on its application, here three protocols are going to be addressed.

3.4.1 Controller Area Network

The protocol Controller Area Network (CAN) was first developed to usage in the automotive field due to the necessity of managing all the information coming from diverse devices as more electronic technology was implemented in vehicles. The CAN protocol is a high-integrity serial bus system for networking intelligent devices able to provide an inexpensive, durable network that helps multiple CAN devices communicate with one another [50].

In the CAN protocol, a message is transmitted to all the devices on the network and each of them decides if that specific message is relevant or if it should be neglected, this characteristic allows to modify a network with minimal impact [50]. The rapid adoption of this protocol occurred thanks to its high scalability, its message priority status and its error handling capabilities, where all of them combined, allows to deliver a message in a correct and non-interrupted way. The CAN buses can be classified into High-speed and Low-speed. The High-speed CAN is by far the most common physical layer and is implemented with two wires and allows communication at transfer rates up to 1 Mbit/s.

Through the years, diverse protocols based on CAN bus have been developed. The CANopen is a high-level communication protocol and device profile specification, developed for embedded networking applications. Each CANopen system (3.5) is made up of one application master and a variable number of slave devices, where every slave in the network is identified unambiguously by means of a 7-bit node address [51].

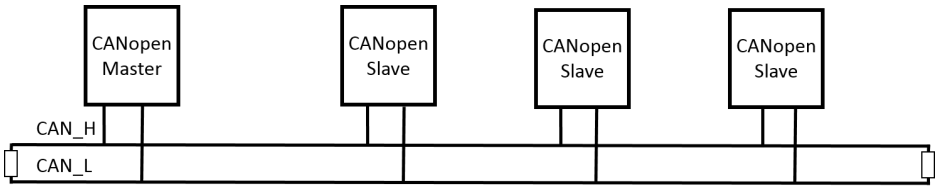

Fig. 3.5 CANopen wiring.

CAN-based networks are used in several fields. Many manufacturers of medical machines have already chosen CANopen as embedded networks [52].

3.4.2 Ethernet

Ethernet was born based on the idea of computers communicating over a shared coaxial cable acting as a broadcast transmission medium and was designed to be flexible and low cost [53], [54]. Ethernet technology provides a set of physical media definitions, a scheme for sharing that physical media and a simple frame format and source-destination addressing scheme for moving packets of data between devices on a LAN [55]. The physical media consist of the electronic devices and hardware needed to carry the digital signals between computers, the scheme in the Ethernet consists of a protocol able to identify when a package had a collision and thus send again the frame corrupted. Finally, the frame consists of shortened pieces of information to be streamed. Each frame contains source and destination addresses, and error-checking data so that damaged frames can be detected and discarded [53]. The Ethernet is characterized by possessing the ability of high capacity where nowadays it is up to 10 Gbps.

3.4.3 Recommended Standard 232

The Recommended Standard 232 (RS232) inception was to help ensure connectivity and compatibility across manufacturers for simple serial data connections. Its strongest application was, and still is, peripheral connectivity for computers. The RS232 protocol consists of a single-ended communication that facilitates the broadcast of data from one sender to one receiver, by adopting a single wire as transmission media and a second one serving as the reference to ground. This characteristic makes this protocol vulnerable to noise, however, it is highly used in low-speed serial communication [56].

Chapter 4

Surgical Robotic Platform for Endoscopic Dissection

Endoscopic procedures for the evaluation and resection of cancerous tissue in the gastrointestinal tract are the preferred option thanks to their small invasiveness and direct access to the area without breaching its natural barriers. At present, the principal endoscopic methods for the resection of polyps in the gastrointestinal tract are endoscopic mucosal resection (EMR), and endoscopic submucosal dissection (ESD) techniques [20]. ESD is a method to remove deep tumors, permitting bloc resection of superficial lesions on the digestive tract and is considered safer and of superior efficacy when compared to EMR [22]. However, ESD is a time consuming and technically demanding method with a probability of 18% of perforating the intestinal wall [37]. Robotics approached have been introduced to address these issues.

The Surgical Robotic Platform for Endoscopic Dissection (RED) was designed as an alternative to tackle the restrictions and drawbacks the ESD technique presents. The RED robotic platform is a novel miniature robotic device for ESD, designed to accurately dissect tumors of the gastrointestinal tract. It has been arranged to be coupled to the tip of the traditional flexible endoscope, thus, exploiting the advantages for navigation in the intestine that a flexible endoscope can offer while enhancing the efficiency of the tissue manipulation thanks to the incorporation of the two-active robotic arms. The advantages of using this robotic device comprise a high operational accuracy, a complete lesion removal warranty, and reduction of costs as this system exploits the locomotion and optics of the flexible endoscope.

Furthermore, a traditional endoscopic room is sufficient to perform a complete surgical operation and the patient does not need to experience surgery under general anesthesia [37].

In this chapter, are exhibited the hardware configuration and mechanical design of the Surgical Robotic Platform for Endoscopic Dissection developed at the Scuola Superiore Sant'Anna. In section 4.1, it is described the overview of the system, while in part 4.2, are listed the diverse hardware components of the system. Lastly, section 4.3 explains the mechanical design of the RED platform.

4.1 System Overview

The Surgical Robotic Platform for Endoscopic Dissection is a robotic system designed to be controlled by two haptic devices (Phantoms). It is composed of two active robotic arms, each with three degrees of freedom, one for gripping the tissue and the other to cauterize it. Furthermore, the robotic platform was designed to enable an adaptable position of the manipulators by introducing two scrollable parts managed by the motors. The scrollable pieces of the robot are contained inside the cap body while on exploration inside the intestine, and once the targeted area is reached they are deployed. The system positioning feedback is directly provided by the endoscope. Fig 4.1 exhibits the prototype of the robotic platform.

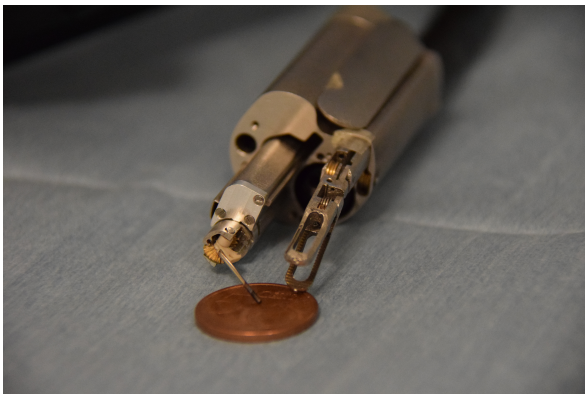

Fig. 4.1 Surgical Robotic Platform for Endoscopic Dissection.

The RED platform exploits the flexibility of the endoscope for navigation and extends the Degrees of Freedom of the conventional endoscope, thus, enhancing the efficiency of complicated tasks. During the procedure, a surgeon will stand near the patient to maneuver

the endoscope. On the other side, another surgeon will conduct the operation utilizing the haptic devices to command the arms of the RED platform.

4.2 Hardware

The Surgical Robotic Platform for Endoscopic Dissection possesses a master-slave configuration and each actuator in the system is responsible for commanding one degree of freedom of one of the tools. The diverse elements composing the RED system are:

- Two Geomagic Touch haptic devices are utilized in the system as the master. This haptic device possesses six-degrees-of-freedom positional sensing and three degree-of-freedom force feedback.
- An Evis exera III gastrointestinal videoscope employed to incorporate the visual feedback.
- A personal computer is in charge of grabbing the information from the haptic devices, process it and transfer the command to the manipulator.
- Six EPOS2 24/2 drivers in charge of receive the information coming from the personal computer and command the motors, all while regulating their velocity, current and position using a cascade of PID controllers.
- One EC6 Maxon motor with Hall sensors and encoder, destined to perform the sliding of the cautery tool.
- Two EC4 Maxon motors with Hall sensors, one executing the yaw movement while the other the pitch one in the cautery tool.
- Three EC22 Maxon motors with Hall sensors and encoders utilized to command the gripper tool. One of the motors holds the task of executing the slide movement, another the yaw while the last one the pitch movement.
- Six external switches to limit the movement of the EC22 motors.
- A power supply of $12A$ and $12V$.
- Actuated cables to transmit the rotational movement from the EC22 motors to the gripper tool.

- A pair of scissors with a potentiometer inside aiming to control the grasp action in the gripper.

4.3 Mechanical Design

The RED platform is conformed by a cap body with two robotic arms (Fig. 4.2). The gripping arm is equipped with a tool to grasp and lift the tissue and it is characterized by possessing three DoFs, *i.e.*, slide, pitch, and open/close of the gripper. The cautery arm is a mono-polar cautery tool also with three DoFs, *i.e.*, slide, roll, and pitch, which is employed to dissect the lesion. The external shape of the cap body is inscribed into a 27*mm* diameter and has a total length of 50*mm*, such defined considering anatomical constraints, *i.e.*, dimension and shape of the intestines. Unlike other NOTES robots, the tendons and sheaths of the RED platform are small enough to be housed within the tool channels of the endoscope, thus, removing the need of a bulking external tube that contains that reduces the steerability of the system [37].

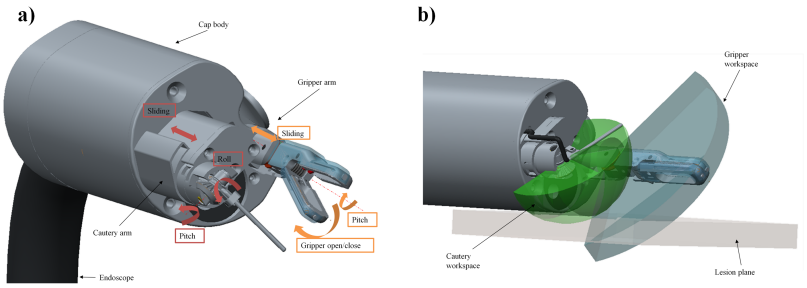

Fig. 4.2 Mechanism of the Surgical Robotic Platform for Endoscopic Dissection.

Fig. 4.3 shows the box that contains the motors in charge of the grasping action and the six drivers controlling the motors. Additionally, this box includes the switches used to limit the displacement of the grasping parts.

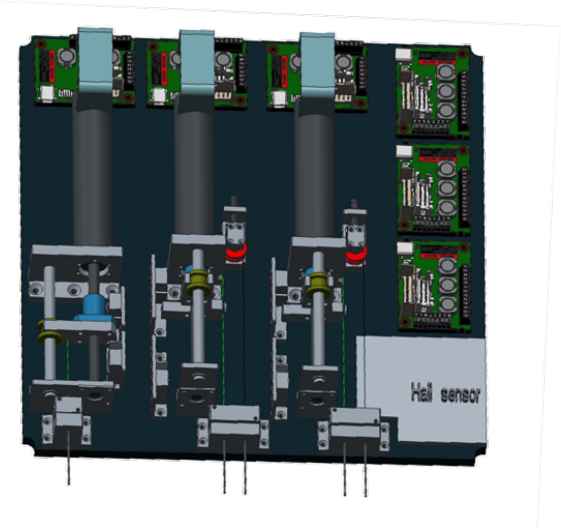

Fig. 4.3 Surgical Robotic Platform for Endoscopic Dissection box.

Chapter 5

Control Design for a Miniaturized Surgical Robotic Platform

The Miniaturized Surgical Robotic Platform for Endoscopic Dissection (RED) in the Gastrointestinal Tract was designed at the Scuola Superiore Sant'Anna aiming to introduce a new approach to dissect cancerous tissue in the gastrointestinal tract. The main objective of this platform was to introduce a system that might resolve the drawbacks encountered in Minimally Invasive methods while exploiting the natural orifices to access the zone of concern. Among the uncertainties of the MIS approaches, we can find the possible port-site metastases or the intricated access to the area of interest due to the anatomical complexity of the gastrointestinal tract, thus the risk of rupture of the natural barriers is always presumable.

This miniaturized robotic system is composed of two haptic devices (masters) which command the tools of the RED system and provide a haptic guide to the surgeons. Then, there is the computer or processing unit which deals with the data and manipulates it to command the motors (slaves) to recreate the action provided by the masters. This scheme is usually implemented in a teleoperated system, and it is known as a master-slave approach. The control design of the robotic platform RED deals with the regulation to provide accurate and fine motion, both to the masters and the slave manipulators, while implementing safety and guidance feedback to the surgeon.

The present study is the extension of the RED project, wherein previous stages the objective was to design the mechanical part of the robotic platform. In the present stage, the scope consists on the projection and implementation of a safe and accurate control system of the RED platform. Section 5.1 gives a general notion of the implementation of the control scheme in the RED platform along with its diverse components. In part 5.2, it is explained the circuit board designed to provide an alternative power supply. Then, section 5.3 illustrates the diverse geometrical abstractions to render the forces in the haptic devices and the pseudo-algorithm. Section 5.4 are exhibits the control simulations of the control loop, that conveniently came along with the EPOS drivers, that are evaluated in terms of performance, and efficiency. Additionally, it is also evaluated, illustrated, and simulated the approach to provide Gain Scheduling to the cascade PI controller. Finally, section 5.5 illustrates the integration of the diverse devices, programming tools, and evaluation of an accurate control implementation.

5.1 System Design Overview

The Miniaturized Surgical Robotic Platform for Endoscopic Dissection is a system involving several components and needs the integration of diverse programming languages that complement each other to achieve a proper execution of the task. Fig. 5.1 depicts the diverse devices and programming tools used to control the RED platform. The control design for this system is a Master-Slave one, where the masters correspond to the two haptic devices, the motors are the slaves, and the computer system represents the control unit which is in charge of the processing and communication between masters and slaves.

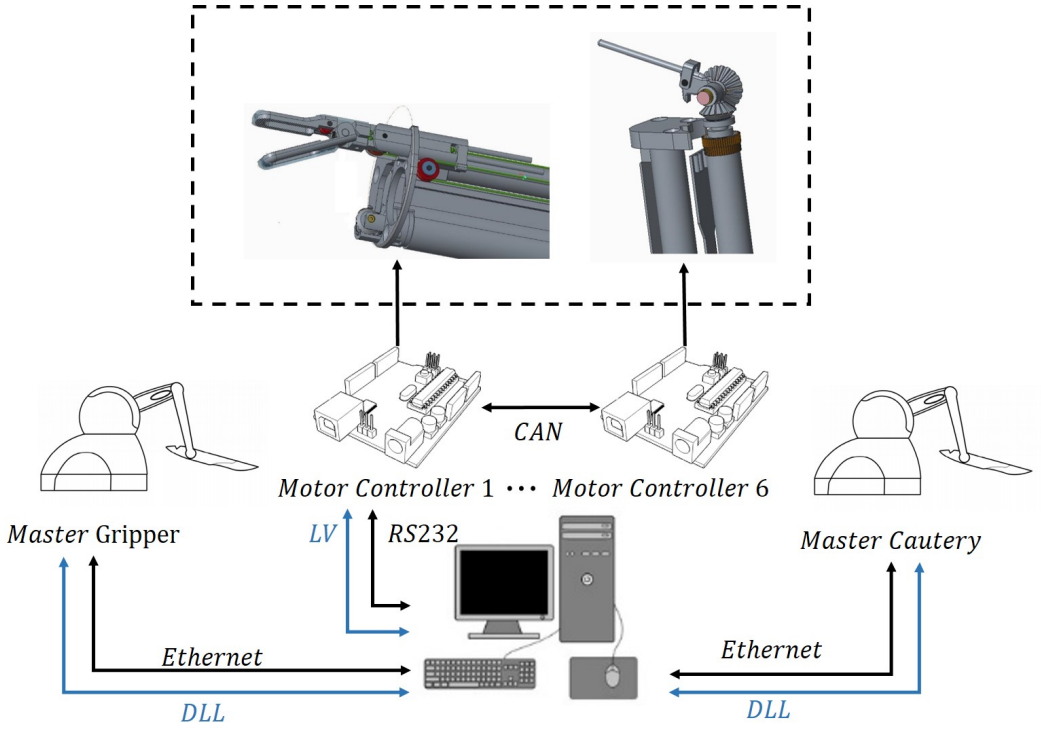

Fig. 5.1 Interaction of the diverse devices used to control the miniaturized robotic system titled RED. In black, it is depicted the communication protocol used to interact with that device while blue expresses the programming tool used to command that specific device.

The design of a control system in Teleoperated platforms is usually approached in a closed-loop structure where the feedback coming from the slaves is frequently regarding the positioning of the tools, and this can be achieved either by an exact position calculation of the end-effector of the robotic slave system or by visual feedback. In the first-mentioned, diverse sensors as encoders, Hall effect and force sensors are needed, which turn out into a bulky system. In the RED platform, the closed-loop is directly chained by the visual feedback of the operator.

To design and incorporate an accurate control scheme to the RED platform, diverse devices and programming languages were integrated. This approach may induce low-time resolution into the system due to the bottleneck generated by the conversion of the *CAN* communication protocol to *RS*232 to enable a proper commanding from the computer. Taken that into account, the use of an Arduino microcontroller was canceled out, which was introduced in the previous stage to manage some inputs and to provide an alternative power supply.

As aforementioned, one of the reasons to include an Arduino platform was to handle inputs. These inputs were needed to notify the system about the mechanical limits of the miniaturized robot and to grab the information coming from a potentiometer integrated into a 3D printed scissors aiming to simulate the grasping of the RED platform. These mechanical limitations are marked for the gripping tool as the three motors used to enable its movement are directly connected to a system of cables, so the amount of cable pulled can be marked and limited by the use of switches; each motor possesses two of them. Fig. 5.2 shows the mechanical approach and position of the switches, that better illustrates what was just mentioned.

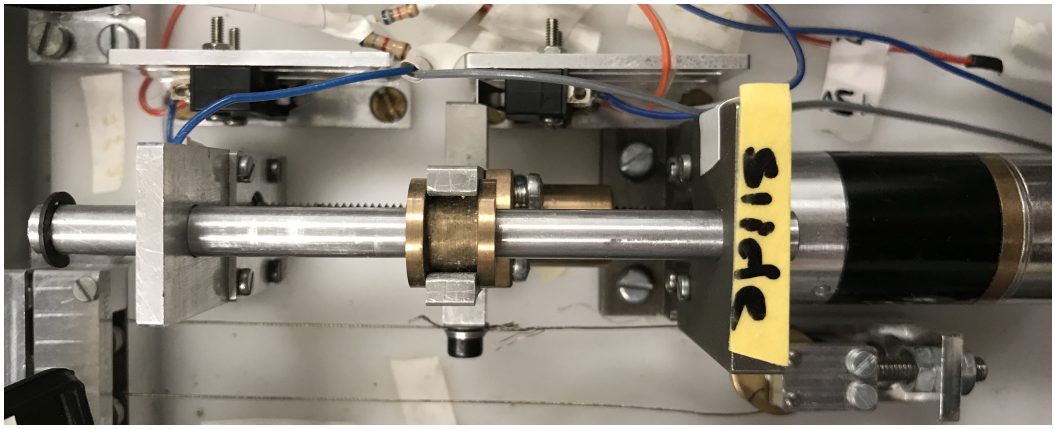

Fig. 5.2 Cable-pull system introduced in the RED platform.

The final configuration and integration of the diverse components involved in the Designed of a control strategy for the RED platform are depicted in Fig. 5.3.

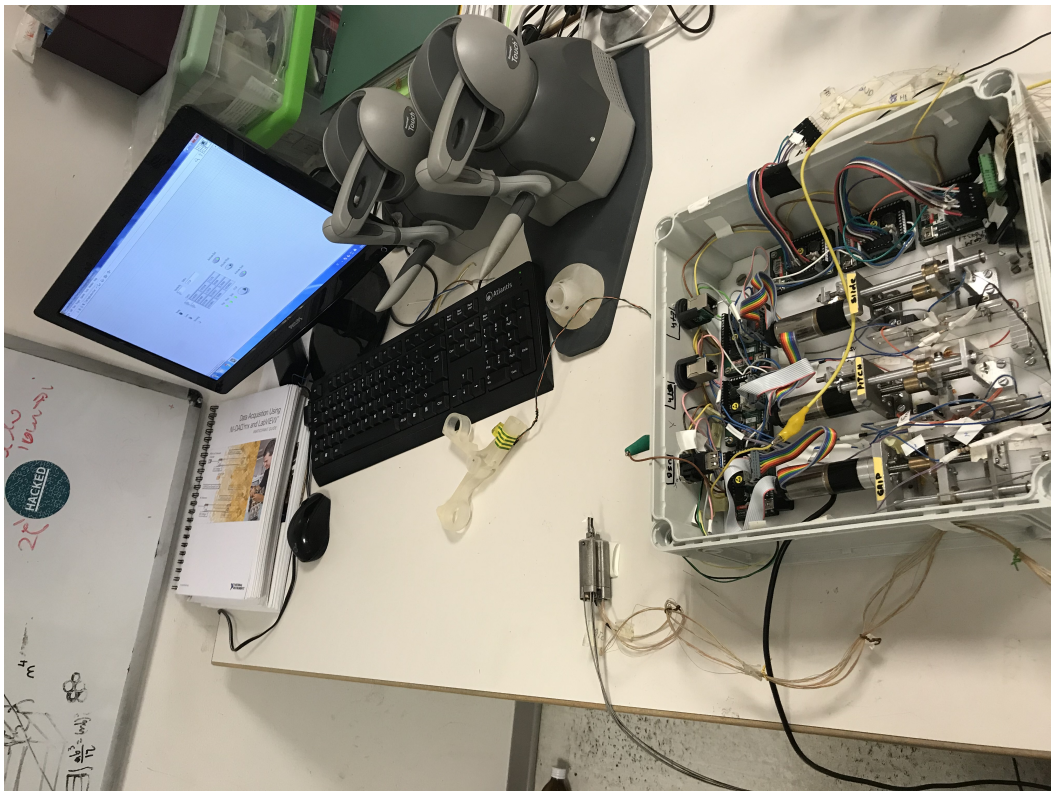

Fig. 5.3 Components of the RED platform.

To develop and design a proper control strategy, diverse steps were followed. Here, a summary is exposed:

1. Hardware improvement.
2. Single motor tuning and commanding through LabVIEW.
3. Motor control modeling on Simulink.
4. Gain scheduling modeling and analysis on Simulink.
5. Development of programming code on C++ to render forces in the haptics devices.
6. Implementation of a Producer/Consumer pattern on LabVIEW where the two haptic devices and an ADC from the EPOS driver are used as the producers.
7. Integration of the motors into the main algorithm. This step was executed by integrating one motor at a time, adjusting its coordinates transformation and sensibility, along

with further programming adjustments to render the control strategy more secure and efficient.

Furthermore, to achieve a similar behavior to the one of the da Vinci platform, the two buttons that are integrated in the phantom device in charge of mastering the cautery tool are used to change the state of the miniaturized robot from an inactive state to an operating one, so to enable re-positioning of the inkwell of the phantoms without affecting or generating any movement in the tools.

5.2 Hardware

The RED platform is integrated by several devices, as already mentioned, and include motors, drives or cable-pull system. Here the approaches and developments utilized to improve the hardware design of the RED platform are introduced.

The *EC*6 motor, which has an encoder integrated, needed for this reason a modification to properly run as the EPOS2 24/2 possesses a pin-out power voltage of $5V$ and the encoder needs $3.3V$ to properly function. In the past, the RED system made use of an Arduino to provide this $3.3V$ to the *EC*6 motor encoder and to use its digital and analog inputs. Differently, in this phase of the RED platform development, the power supply offered by the drivers is exploited, avoiding the inclusion of further instruments than the ones merely needed, thus, improving the determinism of the process as fewer systems are making use of the memory of the computer. Fig. 5.4 shows the schematic design of the voltage and gate conversion of the *EC*6 motor.

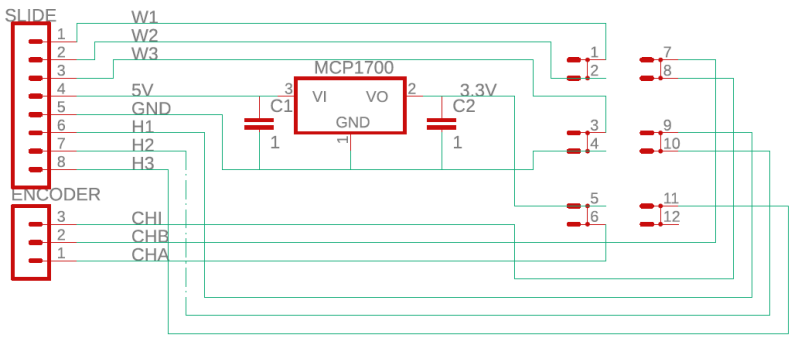

Fig. 5.4 Circuit board design for voltage regulation at encoder of motor *EC*6.

The H depicted in Fig. 5.4 corresponds to the Hall sensors that are incorporated in the $EC6$ Brushless motor for a proper position of the wings, titled W. Furthermore, the encoder channels are represented as CHA, CHB, and CHI. Additionally, the conversion of the power supply from $5V$ to $3.3V$ is also depicted, where this is achieved by implementing a Very Low Dropout Voltage regulator, titled $MCP1700$.

5.3 Haptic Device Control

The Phantom Omni device is a haptic device with three actuated Degrees of Freedom, able to grab the movement of its inkwell and to transform it into Cartesian coordinates, thus, allowing to capture the action made by the user. This section presents the mathematical computations along with the corresponding pseudo-algorithm used to render different forces in this device, where these forces are directly utilized to constrain and manage the diverse types of guidance executed in the present study.

5.3.1 Point Guidance

Among the different types of possible guidance, the point computation consists on constraining the movement of the inkwell about a fixed position or fixed point, thus, the constraints are given in three Degrees of Freedom of the haptic device achieved by computing forces in its three actuated axes. The force imposed could be either attractive or repulsive (See Fig. 5.5), depending on the constant K and the direction of the vector computed between two points, shown in Equation 5.5.

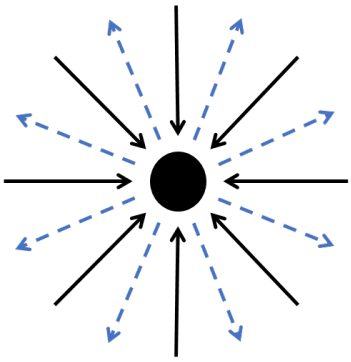

Fig. 5.5 Point guidance.

The actuators presented in the haptic device can be approximated to a damped spring system, thus, the calculation of their force along the three-axis can be simplified and represented as

$$\overrightarrow{F} = K(x - B) \tag{5.1}$$

Where the constant K corresponds to the spring constant, point x is the anchor point and it is precisely at this point where the repulsive or attractive force is applied, and finally, the point B is the current position of the inkwell.

5.3.2 Line Guidance

The line constraining is another haptic guidance type implemented in the control design of the RED platform. A line can be defined by two fixed points, A and C, in a given space. Fig. 5.6b portrays the geometrical approximation used to compute the force along a line, where again, it could be either repulsive or attractive depending on the direction of the computed vector $\overrightarrow{V_d}$.

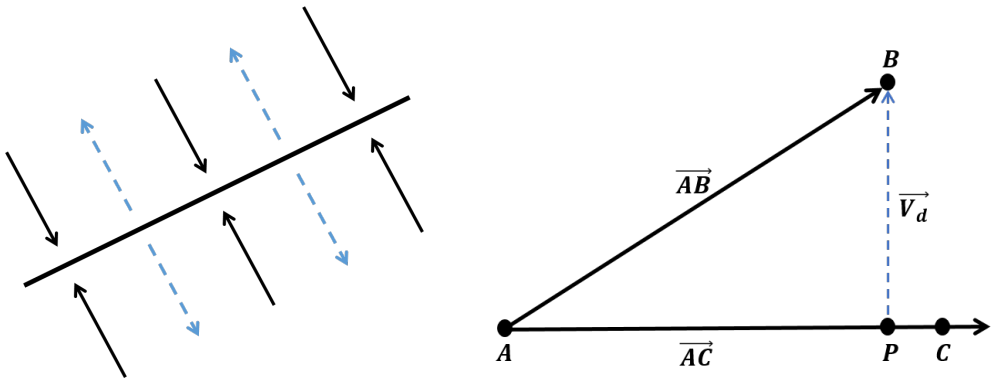

(a) Line force (b) Line vector definition

Fig. 5.6 Line Guidance a) depicts the possible force directions while b) shows the geometrical approach to compute the force rendering of the haptic device.

The current position of the inkwell is depicted in Fig. 5.6b as the point B, and the haptic line guide is defined by points A and C. To compute the corresponding vector orthogonal to the line and passing through point B, it is necessary to calculate the point P that lies on the line and is demarcated as

$$P = A + \gamma(C - A) \tag{5.2}$$

Then, by definition, we have that the dot product of two vectors that are perpendicular to each other is zero

$$(B - P) \cdot (C - A) = 0 \tag{5.3}$$

Replacing the value of P from Equation 5.2 in Equation 5.3 and simplifying it for γ, we have

$$\gamma = (B - P) \cdot (C - A) \tag{5.4}$$

Then the dot product can be drawn as

$$\gamma = \frac{(B - A) \cdot (C - A)}{(C - A) \cdot (C - A)} \tag{5.5}$$

After calculating the distance from A to P, said γ, it is possible to find our final vector $\overrightarrow{V_d}$ which is perpendicular to line defined by the vector $\overrightarrow{AC}$ and passes through points P and B. This vector is established as

$$\overrightarrow{V_d} = \pm(P - B) \tag{5.6}$$

Following, we can estimate the force direction which depends entirely on the direction of the computed vector $\overrightarrow{V_d}$.

5.3.3 Plane Guidance

The last guidance type implemented in the present study is the constraint on a plane. A plane is determined by three points, A, C, and E, as depicted in Fig. 5.7b.

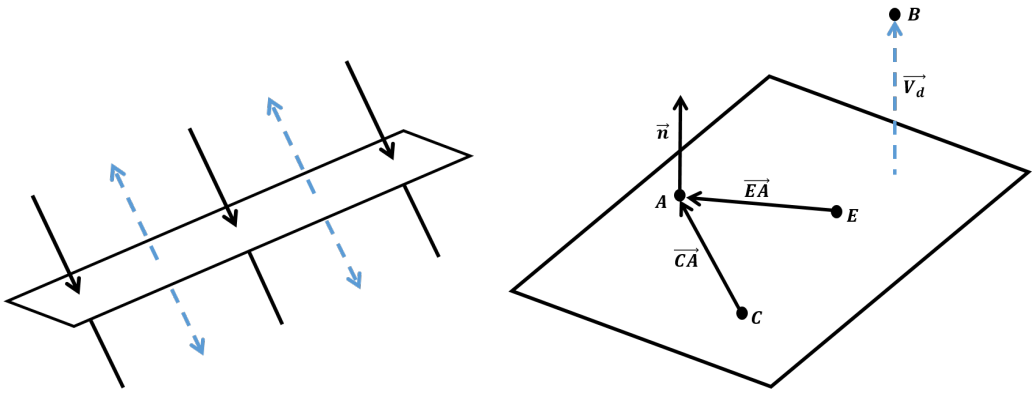

(a) Plane force (b) Plane vector definition

Fig. 5.7 Plane guidance. a) shows the possible fores that can be rendered when constrained in a plane, and b) depicts the geometrical approach in a plane to achieve it.

A plane can be also defined by a vector $\overrightarrow{N}$, orthogonal to the plane, and two points, x and C, that lie on the plane. Again, the dot product between two perpendicular vectors is zero, thus the plane can be denoted as

$$\overrightarrow{N} \cdot (x - C) = 0 \tag{5.7}$$

Then, to find the vector $\overrightarrow{N}$, which is perpendicular to every vector lying on the plane, we define three fixed points A, C and E that reside on the plane and then we compute two vectors as

$$\begin{aligned} \overrightarrow{CA} &= A - C \\ \overrightarrow{EA} &= A - E \end{aligned} \tag{5.8}$$

Then we calculate the cross product between them, where the resulting vector $\overrightarrow{N} =< a, b, c >$ is orthogonal to both of them, thus perpendicular to the plane, and can be expressed as

$$\overrightarrow{N} = \overrightarrow{CA} \times \overrightarrow{EA} \tag{5.9}$$

A plane can also be defined as

$$a(x-x_0)+b(y-y_0)+c(z-z_0)=0 \tag{5.10}$$

And can be simplified as

$$ax+by+cz=d \tag{5.11}$$

Then the deviation e of our point $B=(x_0,y_0,z_0)$, from the plane defined in Equation 5.11 is

$$e=\frac{ax_0+by_0+cz_0+d}{\sqrt{a^2+b^2+c^2}} \tag{5.12}$$

Finally, we can compute our vector $\overrightarrow{V_d}$, which is orthogonal to the plane and passes through point B, as

$$\overrightarrow{V_d}=\overrightarrow{n}e \tag{5.13}$$

Where $\overrightarrow{n}$ corresponds to the vector $\overrightarrow{N}$ normalized.

5.3.4 Algorithm

The algorithm was developed based on the mathematical derivations illustrated in the previous sections, and an overview of its implementation is elucidated on Algorithm 1. This algorithm was developed in C++ and it aims at generating forces in the phantom devices.

Algorithm 1 Haptic forces

Require: *int Hhd*: phantom device identification, *double anchor*: reference point, *double A*: reference point to render force in a line and plane, *double C*: reference point to render force in a line and plane, *double E*: reference point to render force in the plane, *int spring*: spring constant, *int render*: case manager.

Ensure: *int B*1: button one value, *int B*2: button two value, *double pos*: inkwell position, *double ang*: gimbal angles, *double force*: rendered force.

procedure QUERYFORCES($anchor, Hhd, A, C, E, spring, render$)
  $pos \leftarrow inkwell\ position$
  $ang \leftarrow gimbal\ angle$
  $B1, B2 \leftarrow phantom\ buttons\ state$
  if $render = 1$ **then**
    $F \leftarrow spring * (anchor - pos)$
  end if
  if $render = 2$ **then**
    $mag \leftarrow magnitude(anchor - pos)$
    if $mag < 10$ **then**
      $F \leftarrow spring * (anchor - pos)$
    end if
  end if
  if $render = 3$ **then**
    $P \leftarrow A + ((B - A) \cdot (C - A)/magnitude(D))(C - A)$
    $V \leftarrow P - pos$
    if $spring < 0$ **then**
      if $magnitude(V) < 10$ **then**
        $F \leftarrow spring * V$
      end if
    else
      $F \leftarrow spring * V$
    end if
  end if

if $render = 4$ **then**
$N \leftarrow (A-C) \times (A-E)$
$V \leftarrow -N \cdot (A-C)$
$K \leftarrow (N \cdot pos + V)/magnitude(N)$
$n \leftarrow norm(N)$
$point \leftarrow n \cdot K$
$F \leftarrow spring * point$
end if
$renderF$
return $pos, ang, F, B1$ and $B2$
end procedure

The options on Algorithm 1 to provide diverse guidance types are managed by the render variable. If the value of *render* is equal to zero, the haptic device only delivers information about the inkwell, and angle position, thus, no force is generated. Another case is when the *render* variable is equal to one (See line 5), where the information regarding the position is equally gathered, but also the is a force generation on the selected phantom towards or outwards a defined point on its operating space, where this depends on the value of the spring constant. Then, a similar case is when *render* is equal to two but the force is only generated if the inkwell is withing a range of $10mm$ of the given point (See line 8). Another distinct case, is when the variable is equal to three (See line 14), where a force is developed in a given line. Finally, if the variable *render* is equal to four, the guidance type in the plane is activated (See line 25).

5.4 Motor Control

A brushless DC motor, as explained in previous chapters, is a motor that is usually composed of three wings, and their orientation and displacement are determined by integrated Hall sensors. The control of velocity and direction of the movement of this type of motors is achieved by designing circuits that allow controlling the amount of current, tension, and time to achieve the desired behavior. In this study, that step was avoided by including in the system an already built driver, titled EPOS2 24/2, that fits the objectives of the project to control accurately the position and to provide the current needed to achieve a good performance.

This driver comes with an integrated cascade PID control that allows managing the current, position, and velocity of the motors. Furthermore, the Maxon driver can be tuned using a software tool that allows calculating the PID parameters according to the plant, its response, and the type of motor we are dealing with, meaning that this tuning process is responsible for optimizing the system response. Moreover, the tuning process must be performed considering the complete system inertia to allow an accurate system identification. The steps to accomplish the tuning process of each motor by the EPOS Studio software are:

1. Identification of the plant.
2. Calculation of PID parameters.
3. Verification.

However, to test and verify the cascade PID performance when there are fluctuations in the velocity or more importantly, under constantly fluctuating load as characterizes the RED system, were built in Simulink the cascade models that are integrated with the EPOS driver.

5.4.1 Motor Control Models

When modeling a brushless DC motor, there are different approaches to accomplish it, and it is needed to consider their electrical and mechanical characteristics. Here, the models provided by Maxon are utilized. In the plant model of the motor, as it is commonly done, the nonlinear effects are neglected, and the linear transfer function is built based on the input-output response.

The modeling stage was introduced as this type of motor is highly sensitive to current variations and any over-current can damage it. Therefore, the principal aim to model the cascade PI control is to check its ability to control the current that fluctuates depending on the load and torque requirements. Fig. 5.8 depicts the model of the brushless model, which was implemented in Simulink.

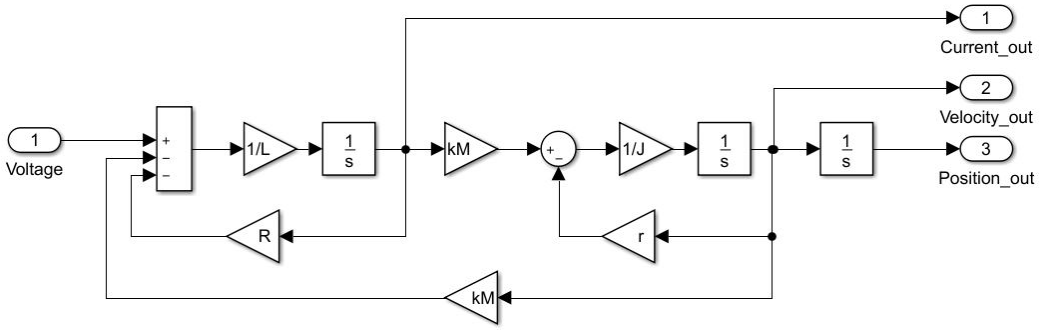

Fig. 5.8 Model of the motor plant.

Where K_M corresponds to the torque constant and it is the interface between the electrical and mechanical parts of the model, J is the inertia of the motor rotor and the load, L is the inductance phase to phase, R is the resistance phase to phase, and r represents to the load.

The cascade PI control included in the EPOS driver is composed of a current loop, a velocity regulation, and a positioning regulation loop. Here, are explained the models corresponding to the current and velocity loops. The principal regulation structure corresponds to the current control, as during the movement must be regulated the torque and forces of the motor. Fig. 5.9 illustrates the PI control model, where the block titled plant represents the model of the motor (See Fig. 5.8).

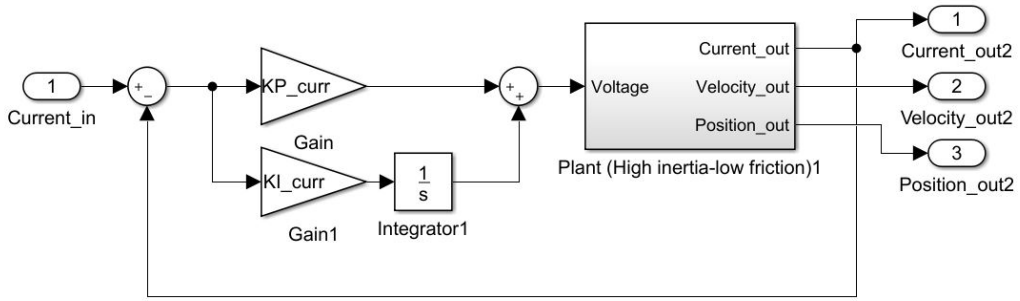

Fig. 5.9 Current PI model control.

Then, the velocity regulation loop (See Fig. 5.10) was built, where inside its structure there is the current regulation loop, which controls the amount of current provided to the motor according to the amount required by the velocity loop.

$$\tau = IK_M \tag{5.14}$$
$$\tau = \frac{V - \omega K}{R} K$$

Where V represents the voltage, I is the armature current, K is the motor constant, ω embodies the rotational speed, and τ is the torque. As can be seen from Equation 5.14, when there is an increase in the rotational speed there is also a reduction in the torque, as the others variables are constant. Then, it can be said that there is a relation between the speed and the current in the system, as the model in Fig. 5.10 expresses.

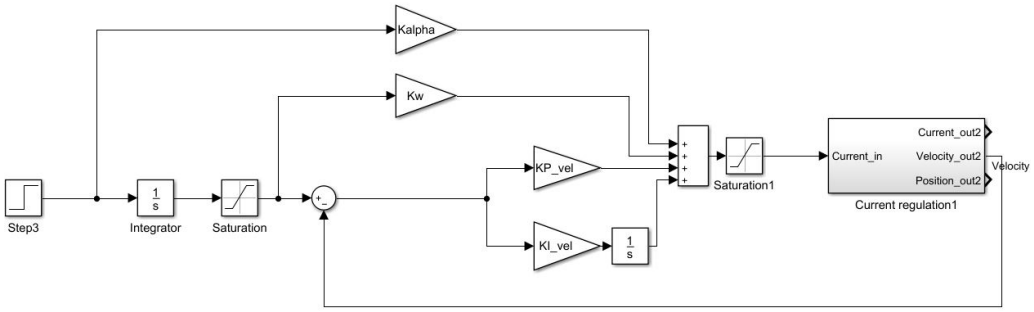

Fig. 5.10 Velocity cascade PI control model.

Where K_ω provides an additional amount of current in cases where the load increases with the speed and K_α provides more current in cases of high acceleration or high load. In this model, the value of K_ω is small and the one of K_α is zero. The values of the Proportional and Integrative parameters of all the cascade PI control are the ones given after tuning the drivers with the EPOS Studio tool.

5.4.2 Fuzzy Gain Scheduling of PID

The Gain scheduling PI algorithm is a method that allows adjusting the gains of the PI controller, depending on the input error. Even though the EPOS Studio tool makes use of plant identification, simulating diverse frequencies and loads, the PI control structure is by itself an approach that does not performance as desired in nonlinear cases. This is especially relevant in the case of motors that do not have integrated encoders, as the block commutation

generates abrupt switching of the current every 60 degrees and the PI regulation might not be sufficient. Therefore, the fuzzy Gain scheduling is proposed as a method that might reduce this drawback and augment the performance of the already well functioning controller.

The Gain scheduling algorithm is based on fuzzy logic, where the first step to build it is to define the membership functions (MFs). Fig. 5.11 depicts the membership functions utilized in the inputs and outputs of the fuzzy logic.

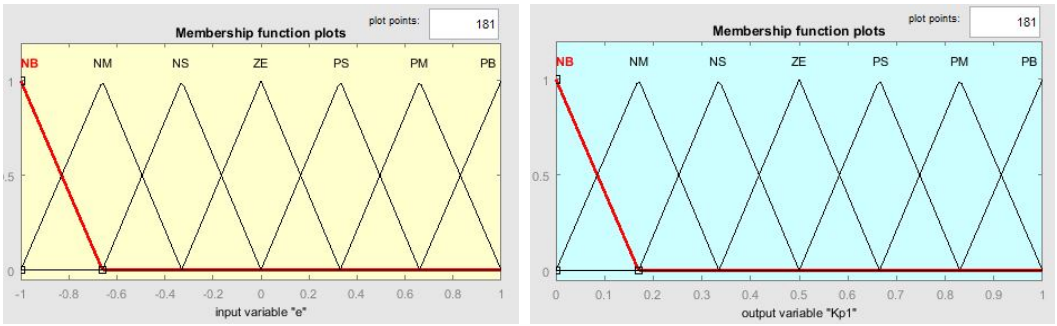

(a) Input (b) Output

Fig. 5.11 a) shows the membership functions (MFs) of the fuzzy algorithm for the input parameters, error and its derivative, while b) the ones of the output parameters, PI parameters.

Then, Fig. 5.12 depicts the rules that define the way the parameters gain need to be adjusted depending on the value of the inputs. Aiming to simplify the interpretation, only the surface of the parameters is depicted and not the entire 49 rules table.

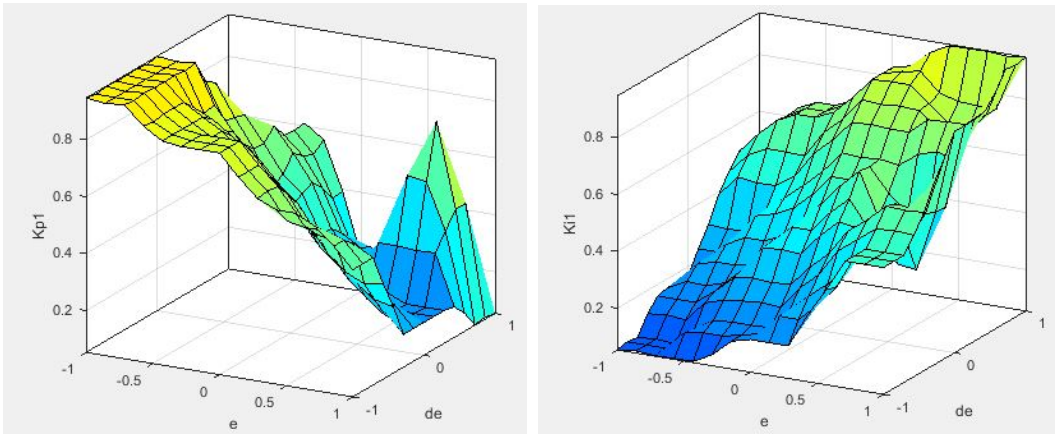

(a) Proportional parameter. (b) Integrative parameter.

Fig. 5.12 a) shows the rules surface of the fuzzy algorithm for the Proportional (P) parameter, and b) depicts the one of the Integrative (I) parameter.

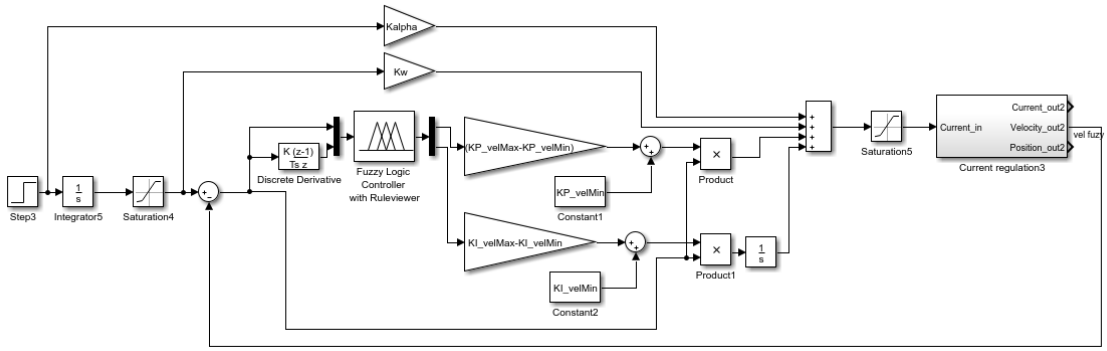

Fig. 5.13 Velocity cascade PI control model with Gain Scheduling.

The integration of the Gain scheduling is based on the derivations explained in section 2, where it should be remembered that there is a normalization of the obtained value, so the concluding value of the parameter belonging to the velocity loop is going to vary around the value found via the EPOS Studio tool, thus, the minimum performance of the regulator is guaranteed.

5.4.3 Results

In this section, are elucidated the results obtained from the tuning process of the EC22 motor as well as the simulations of the cascade PI controller compared to the outputs gather from the Gain scheduling approach. Fig. 5.14 depicts the position and current output of the cascade PI controller, where it is evident the need to introduce a method that allows controlling further the behavior of the current.

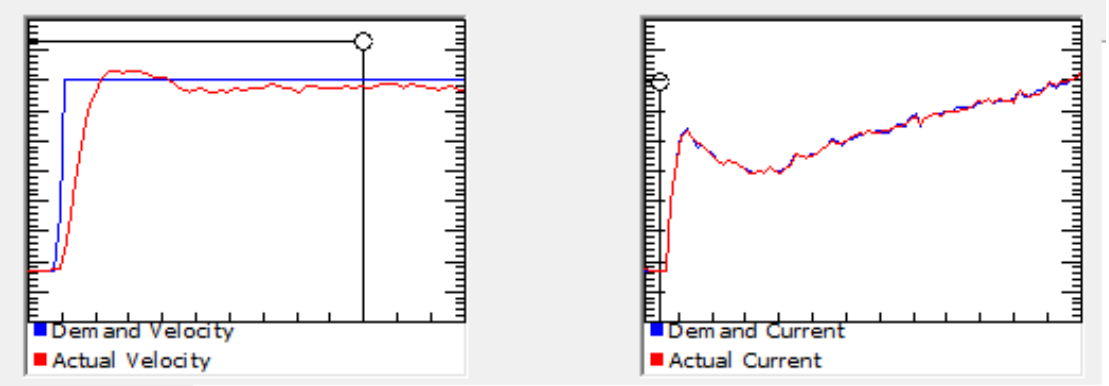

Fig. 5.14 EPOS Studio tuning results of one EC22 motor. The graph on the left corresponds to the position results while the one on the right, is the current loop behavior.

As explained in the previous sections, the current control is the most interesting regulation loop for the current study, as a poorly current control can damage the motors. Furthermore, the regulation over the position is not fundamental, as the main positioning feedback which is the visual one, is not accurate, besides the task that the RED platform will be in charge of does not require this feature. Fig. 5.15 depicts the output value of the current loop when there is a step function in the input and a load at time $2s$. The output value of the fuzzy gain scheduling is illustrated in red while the response of the simple PI current loop is depicted in yellow.

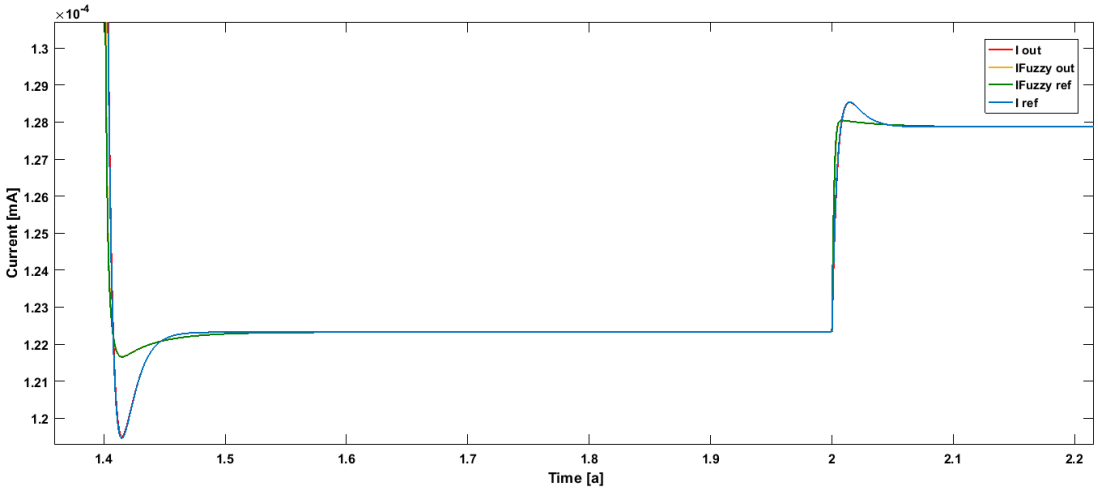

Fig. 5.15 Current output comparison of the cascade PI model vs the cascade PI model with Gain Scheduling.

Finally, the velocity output of both approaches was gathered and compared. Fig. 5.16 shows the response of both methods when exposed to the same load at the very same time. There is a faster adaptation, lower overshoot, and higher time response in the fuzzy logic approach compared to the cascade PI controller. However, it must be taken into account that the non-linearities of the model were omitted, thus it is expected a more fluctuating response when testing in the real system.

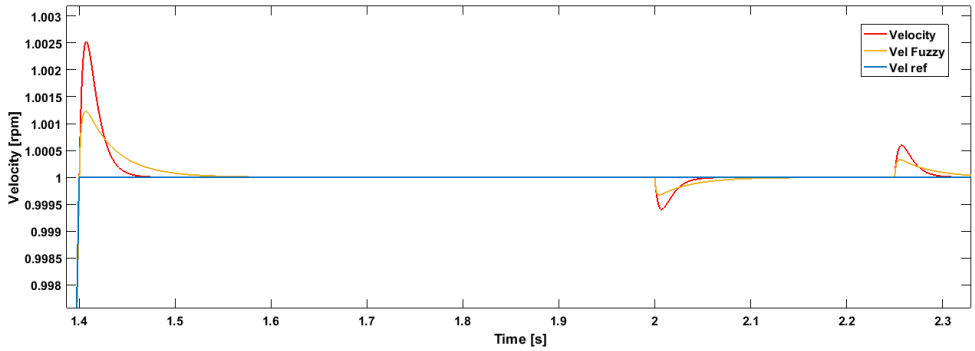

Fig. 5.16 Velocity output comparison of the cascade PI model vs the cascade PI model with Gain Scheduling.

5.5 Integration and Control Program

In this section, the details regarding the security and steps followed to implement and test the designed scheme are explained. The integration part comprehends all the steps and algorithms needed to achieve a safe control scheme able to provide haptic guidance to the operator along with notifications regarding the state of the devices used. The test part corresponds mainly to the verification of the proper development of tasks. The steps followed to develop the control scheme of the RED platform were:

1. DLL to render forces in the haptic devices.
2. Motor tuning and LabVIEW control.
3. Design of producer/consumer pattern on LabVIEW, using the phantoms as the devices producing the information.
4. Integration of ADC as the second producer.
5. Design of the state machine.
6. Clean and manage data when there is a change in the states.
7. Introduction of the buttons to manage the states.
8. Incorporation of one motor and adjustments on the sampling frequency.

9. Error handling.
10. User interface.
11. Over-current protection.
12. Transformation of coordinates from phantom to relative movement to the motor.
13. Movement of one motor according to the displacement given by the phantom and adjustments.
14. Managing of the switches signaling the mechanical limits.
15. Implementation of one motor at a time, while adjusting their movement sensibility.
16. Development of the Stop state to take the system into its home state.

Next, is elucidated the algorithm and a broader explanation of the main control development.

5.5.1 Main program

The main program, developed in LabVIEW, controls and combines the diverse devices that integrate the RED platform. This algorithm is based on a producer/consumer pattern and has a sampling frequency of $1kHz$, one while loop for the producer and two consumer loops. The producer loop gathers the information coming from the operator while the consumers are in charge of taking an action depending on the values sent by the producer.

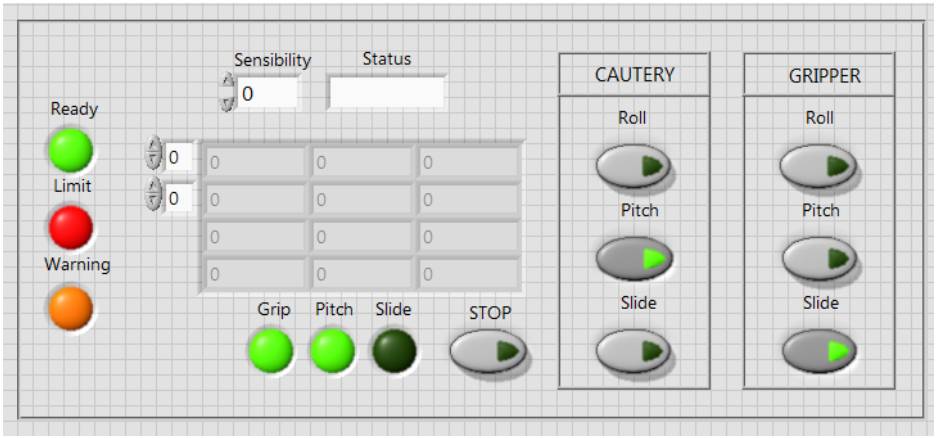

Fig. 5.17 LabVIEW user interface.

On start, it is rendered an attractive force towards a defined point in the cartesian space of the phantom, and the systems enter into an inactive state. Then, the system waits for input generated by the user, and this is interfaced through the two buttons integrated into the phantom, which manage the state machine inside the consumer loops. This state machine is composed of three possible states: Inactive, Operating and Stop. The Inactive state allows the user to accommodate the tools without introducing any movement into the robotic system. In the Operating state, as its name states, there is an interaction between the operator and the tools. Finally, the Stop state is activated when the operator decides to terminate the operation and click the button that lies in the user interface (See Fig. 5.17). This particular state takes the RED gripping tool to an initial position, all controlled by the switches that are held in the box containing the motors, where first the gripping is closed, then the pitch is brought to the home position, and finally, the sliding turns too to its initial arrange. Moreover, the interface allows to enable and disable the selected motors, offering a higher control to the operator depending on its necessities. Additionally, the interface possesses three LEDs that alert the operator regarding the states of the tools. The Ready LED, notify the moment in which the system is ready to operate, the Limit one provides alerts regarding the mechanical limits of the gripping tool, and the Warning LED suggests the user be careful with the operation that is being held, as there is a probable over-current in one of the motors. An overview of the main program is elucidated on Algorithm 2.

Algorithm 2 Main algorithm based on a Producer/Consumer pattern

Initialize:
Render attractive force towards a point in phantoms
Initialize motors
$State \leftarrow Inactive$
procedure PRODUCERS
    while $Stop \neq 1$ **do**
        $position \leftarrow produce$ inkwells and gimbals positions
        $ADC \leftarrow produce$ gripping position
        Put ADC in buffer $bf1$
        Put $position$ in buffer $bf2$
        $B1 \leftarrow cautery$ button 1
        $B2 \leftarrow cautery$ button 2
        $Stop \leftarrow Stop$ button on interface
        if $B1 = 1$ **then**
            $State \leftarrow Run$
            render attractive force in a line
        end if
        if $B1 = 1$ **then**
            $State \leftarrow Inactive$
            render attractive force in a line
        end if
        if $Stop = 1$ **then**
            $State \leftarrow STOP$
        end if
    end while
end procedure
procedure CONSUMER 1
    while $Stop \neq 1$ **do**
        $ADC \leftarrow bf1$ and remove item from buffer $bf1$
        if $State = Inactive$ **then**
            stop movement and wait until change of state
        end if

```
33:         if State = Run then
34:             if Previous State = Inactive then
35:                 wait 5 loop iterations to move motors
36:             else
37:                 diff ← positionNow − positionPrev
38:                 transform diff to relative motor movement
39:                 if MotorCurrent < Limitcurrent then
40:                     if SW1 ≠ 1 and SW2 ≠ 1 then
41:                         move motor to relative position
42:                     else
43:                         move motor to opposite direction of the limit switch
44:                         and emit alert through user interface
45:                     end if
46:                 else
47:                     stop movement and emit alert through user interface
48:                 end if
49:             end if
50:         end if
51:         if State = STOP then
52:             stop movement of motors
53:             while SW1 ≠ 1 do
54:                 move EC22 gripper motor towards home position
55:             end while
56:             bandADC = 1
57:             close motor channel
58:         end if
59:     end while
60: end procedure
61: procedure CONSUMER 2
62:     while Stop ≠ 1 do
63:         position ← bf2 and remove item from buffer bf2
```

```
64:     if State = Inactive then
65:         stop movement on motors and wait until change of state
66:     end if
67:     if State = Run then
68:         if Previous State = Inactive then
69:             wait 5 loop iterations to move motors
70:         else
71:             diff ← positionNow − positionPrev
72:             if MotorCurrent < Limitcurrent then
73:                 if EC22 motor = True then
74:                     transform diff to relative motor movement
75:                     if SW1 ≠ 1 and SW2 ≠ 1 then
76:                         move motor to relative position
77:                     else
78:                         move motor to opposite direction of the limit switch
79:                         and emit alert through user interface
80:                     end if
81:                 else
82:                     transform diff to relative motor movement
83:                     move motor to relative position
84:                 end if
85:             else
86:                 stop movement and emit alert through user interface
87:             end if
88:         end if
89:     end if
90:     if State = STOP then
91:         stop movement of motors
92:         while bandADC ≠ 1 do
93:             wait
94:         end while
```

```
95:             while SW3 ≠ 1 do
96:                 move EC22 grip motor towards home position
97:             end while
98:             while SW5 ≠ 1 do
99:                 move EC22 slide motor towards home position
100:            end while
101:            close all motor channels
102:        end if
103:    end while
104: end procedure
```

Algorithm is based on a producer consumer pattern, where the add and remove functions were excluded. Both of them are needed to manage the synchronization and to make the producer and consumer be aware when the buffer is full or empty, which is the principle of a producer consumer pattern, to keep the data and to consume it only if there is data in the buffer. However, as in the LabVIEW algorithm that uses this pattern, a enque form that only keeps the most recent information is used so to improve the time resolution. The pattern was used to reduce the possible amount of data lost and make the movement smoother but the synchronization of the producers inputs with the consumer is high.

5.5.2 Coordinates Transform

The haptic devices are the master agents in the RED platform, thus, appropriate management of their data and its transformation is fundamental to command the motors as desired by the operator. The phantoms possess three-axis that execute the macro movements, and three more that perform the pitch, roll, and yaw that are the reference to the movements of the gimbal. The resolution of the macro movements bears a value of $r_{phant} = 0.055mm$, while that of the other three axes, is not given.

Regarding the EPOS motors, they can be set in a mode to move towards a relative position, where the input is the number of steps to complete, and the direction is indicated by a plus or minus sign. Equations 5.15 illustrates the approach used in this study to transform the data from the inputs (ADC and phantoms) into a relative movement of the motors.

$$x_{motor} = K\Delta x \tag{5.15}$$
$$\Delta x = pos_{new} - pos_{old}$$

Where pos_{new} corresponds to the most recent acquired value from the phantom and pos_{old} is the value obtained five iterations ago. The value of K is a constant which depends on the motor type and the information we are gathering (macro movements, gimbal or ADC). In the case of the macro movements, we have

$$K_{macro} = \frac{r_{motor}}{r_{phant}} \tag{5.16}$$
$$r_{motor} = \frac{\phi_{rotor} \times \pi}{qc_{turn}}$$

While for the movements of the gimbal and ADC, as no resolution is provided, the K constant is derived as

$$K_{gimbal/ADC} = \frac{qc_{turn}}{lim_{max} - lim_{min}} \tag{5.17}$$

Where qc_{turn} represents the states per turn of the motor and the lim variables, the upper and lower limit of the phantom, where

$$-1.45 < pitch < 1.05$$
$$-2.66 < roll < 2.16$$
$$1660 < ADC < 2530$$

and

$$EC_4 : qc/turn = 6$$
$$EC_6 : qc/turn = 2000$$
$$EC_{22} : qc/turn = 2048$$

Then, as the information comes from devices that are subjected to variations even though no command is given to them, a range of variation to reject a given data was defined, where for the ADC Δx is of 3, for the gimbal Δx of 0.0015, and the macro movements of 12. Then, a gain value was implemented in each transformation to augment its sensibility and to fit this derived data with the mechanical design.

Chapter 6

Discussion, Conclusions and Recommendations

6.1 Discussion

The diverse modes of haptic guidance allow the operator to recreate a more comfortable and realistic environment to perform the surgery. Each of them provides advantages and their use depends on the required application, as long as the possible preferences of the operator. Indifferent to the guiding type, the implementation of guidance feedback has proven to provide an accurate guide to surgeons. Furthermore, it will enable the implementation of force feedback at the tip of the tools, after a sensor system is implemented in the RED platform.

In this application, gears and cable-pulled systems are used to transform the motor rotation into either linear or rotational movement. However, exists an associated elasticity and backlash of these parts, creating an effect of compliance, thus, a delay in the drive chain and the plant itself is also generated. Such delay influences the regulation stability, affecting the accuracy of the PID control. To overcome these limitations, it would be necessary to introduce in the system sensors able to provide feedback regarding the load movement. However, new control approaches might bring alternatives to solve such drawbacks.

The Gain Scheduling algorithm is based on the fuzzy logic to adapt the gains of PIDs controllers, so they allow to exploit of the well-known advantages of these regulators while improving their adaptability to nonlinearities. The fuzzy PI Gain Scheduling algorithm was studied to propose a solution to the backlash drawback presented in the RED platform, along with a possible augmentation of the adaptability of the cascade PI regulation scheme that was already built in the Maxon driver. It should be noted that every effort to improve the control stability and to regulate the current flowing through the motors is valid, as poor management can damage the motors, which would need their replacement in a system where its mechanical assembly is quite delicate and time-consuming.

The resulting simulations of the Gain Scheduling PI were integrated into the velocity loop of the cascade PI, and its accuracy was compared with the one of the velocity control without a Gain Scheduling. The designed fuzzy based algorithm shows a higher performance as its simulations hold higher time response, lower overshoot, and lower variation when there is a sudden load in the system. Experiments must be compassed to check its feasibility, and then incorporate this method into the RED platform.

Regarding the accuracy and stability of the control system, the adoption of the PC as the processing unit has proven to be sufficient as the producer/consumer pattern allows the storage of information, thus, diminishing the amount of data loss. Additionally, the timing necessities in the RED system are successfully covered by this processing unit. However, to render the control system more reliable, it is necessary to reduce the number of processes being executed at the same time, to increase the amount of available memory to execute accurately the control program of the RED platform.

6.2 Conclusions

The haptic guidance that enables the interaction of the surgeon-robotic platform is potentially valuable as it allows the operator to adapt easier, and learn faster how to control the system, all while reducing the error as the environment is more controlled. However, haptic feedback to provide information regarding the produced forces due to interaction with the tissues is needed to render the platform more efficient and make it more appealing to the health care specialists.

A consumer/producer pattern has proved to be efficient in terms of accuracy, precision, and safety of the data. Furthermore, the possibility of managing diverse frequencies in

the producer and consumer loops are desired when introducing asynchronous systems. Additionally, this pattern does not occupy an enormous space in the memory which seems ideal in the systems where the processing unit does not process the information in real-time, as it is the RED platform.

Furthermore, the reduction of hardware and software, when designing control schemes, must be a theme of great attention as the memory use should be constrained. Moreover, the reduction of devices incorporated in a system diminishes also the probability of failure, which is desired to keep the system reliable and safe.

A cable-pull system is a good option when building reduced sized robotic platforms. However, this approach presents the backlash drawback and for interventions that need high positioning resolution, this method is not the best option. Indifferent to this obstacle, this method fits perfectly in the RED platform as the task itself does not demand high positioning resolution, and the visual feedback to control velocity, and position is sufficient.

Finally, as a remark, any effort to improve or develop new platforms is worthwhile as it will open new gates regarding the way the gastrointestinal interventions are going to be approached, thus, leading to the expansion and exploration of methods to solve the obstacles in this field.

6.3 Future Work

In future works, haptic feedback is proposed as an approach to provide a sensory interface of the forces imposed at the tip of the tools. To do so, a conjunct of sensory devices must be incorporated into the RED platform. Additionally, to solve the backlash and nonlinearities adaptation of the regulation approach in the motors, it is proposed to incorporate and evaluate the Gain Scheduling algorithm here derived.

Finally, to assess the accuracy of the RED platform, trials with surgeons are proposed. Further tests are proposed to evaluate the assessment of the haptic guidance while on test on a phantom of the gastrointestinal tract. Then, an adjustment phase of the RED robotic system based on the feedback given by the health care specialist will be necessary as well.

6.4 Recommendations

The first recommendation, and maybe the principal drawback found in the development of the control system of the RED platform, consists of providing a guide that elucidates the developments implemented, and the way everything is integrated, so future works can be materialized in a faster and more efficient way.

Additionally, when designing the control system of a platforma key part is to keep it simple and work most efficiently, always looking to reduce the number of objects in the system. Finally, a desired step when designing control strategies is to simulate the system and identify possible complications or drawbacks that the approach being proposed can bring.

References

[1] Koichi Suda, Masaya Nakauchi, Kazuki Inaba, Yoshinori Ishida, and Ichiro Uyama. Minimally invasive surgery for upper gastrointestinal cancer: Our experience and review of the literature. *World journal of gastroenterology*, 22(19):4626, 2016.

[2] World Health Organization. Cancer. Technical report, 2018.

[3] Valentina Vitiello, Su-Lin Lee, Thomas P Cundy, and Guang-Zhong Yang. Emerging robotic platforms for minimally invasive surgery. *IEEE reviews in biomedical engineering*, 6:111–126, 2012.

[4] Elena Ortiz-Oshiro, Iris Sánchez-Egido, Jesús Moreno-Sierra, Cristina Fernández Pérez, Jesús Sánchez Díaz, and Jesús Álvarez Fernández-Represa. Robotic assistance may reduce conversion to open in rectal carcinoma laparoscopic surgery: systematic review and meta-analysis. *The International Journal of Medical Robotics and Computer Assisted Surgery*, 8(3):360–370, 2012.

[5] Oded Zmora and Eric G Weiss. Trocar site recurrence in laparoscopic surgery for colorectal cancer: myth or real concern? *Surgical oncology clinics of North America*, 10(3):625–638, 2001.

[6] Myriam J Curet. Port site metastases. *The American journal of surgery*, 187(6):705–712, 2004.

[7] Guoxin Fan, Zhi Zhou, Hailong Zhang, Xin Gu, Guangfei Gu, Xiaofei Guan, Yunshan Fan, and Shisheng He. Global scientific production of robotic surgery in medicine: a 20-year survey of research activities. *International Journal of Surgery*, 30:126–131, 2016.

[8] Stavros A Antoniou, George A Antoniou, Oliver O Koch, Rudolf Pointner, and Frank A Granderath. Robot-assisted laparoscopic surgery of the colon and rectum. *Surgical endoscopy*, 26(1):1–11, 2012.

[9] Manish M Tiwari, Jason F Reynoso, Amy C Lehman, Albert W Tsang, Shane M Farritor, and Dmitry Oleynikov. In vivo miniature robots for natural orifice surgery: State of the art and future perspectives. *World journal of gastrointestinal surgery*, 2(6): 217, 2010.

[10] Michael J Mack. Minimally invasive and robotic surgery. *Jama*, 285(5):568–572, 2001.

[11] KH Fuchs. Minimally invasive surgery. *Endoscopy*, 34(02):154–159, 2002.

[12] Keisuke Koeda, Satoshi Nishizuka, and Go Wakabayashi. Minimally invasive surgery for gastric cancer: the future standard of care. *World journal of surgery*, 35(7):1469–1477, 2011.

[13] HD Hoeg, A Brett Slatkin, Joel W Burdick, and Warren S Grundfest. Biomechanical modeling of the small intestine as required for the design and operation of a robotic endoscope. In *Proceedings 2000 ICRA. Millennium Conference. IEEE International Conference on Robotics and Automation. Symposia Proceedings (Cat. No. 00CH37065)*, volume 2, pages 1599–1606. IEEE, 2000.

[14] Marianne Ashford. Gastrointestinal tract–physiology and drug absorption. *Aulton's pharmaceutics e-book: the design and manufacture of medicines*, page 300, 2017.

[15] Pietro Valdastri, Massimiliano Simi, and Robert J Webster III. Advanced technologies for gastrointestinal endoscopy. *Annual review of biomedical engineering*, 14, 2012.

[16] Fábio Shiguehissa Kawaguti, Caio Sérgio Rizkallah Nahas, Carlos Frederico Sparapan Marques, Bruno da Costa Martins, Felipe Alves Retes, Raphael Salles S Medeiros, Takemasa Hayashi, Yoshiki Wada, Marcelo Simas de Lima, Ricardo Sato Uemura, et al. Endoscopic submucosal dissection versus transanal endoscopic microsurgery for the treatment of early rectal cancer. *Surgical endoscopy*, 28(4):1173–1179, 2014.

[17] Divyanshoo R Kohli and John Baillie. How endoscopes work. In *Clinical Gastrointestinal Endoscopy*, pages 24–31. Elsevier, 2019.

[18] Kamal Nagpal, Kamran Ahmed, Amit Vats, Danny Yakoub, David James, Hutan Ashrafian, Ara Darzi, Krishna Moorthy, and Thanos Athanasiou. Is minimally invasive surgery beneficial in the management of esophageal cancer? a meta-analysis. *Surgical endoscopy*, 24(7):1621–1629, 2010.

[19] HG Beger, A Schwarz, and U Bergmann. Progress in gastrointestinal tract surgery: the impact of gastrointestinal endoscopy. *Surgical Endoscopy and Other Interventional Techniques*, 17(2):342–350, 2003.

[20] Sergey V Kantsevoy, Douglas G Adler, Jason D Conway, David L Diehl, Francis A Farraye, Richard Kwon, Petar Mamula, Sarah Rodriguez, Raj J Shah, Louis Michel Wong Kee Song, et al. Endoscopic mucosal resection and endoscopic submucosal dissection. *Gastrointestinal endoscopy*, 68(1):11–18, 2008.

[21] Gregory Y Lauwers, David G Forcione, Norman S Nishioka, Vikram Deshpande, Mikhail Y Lisovsky, William R Brugge, and Mari Mino-Kenudson. Novel endoscopic therapeutic modalities for superficial neoplasms arising in barrett's esophagus: a primer for surgical pathologists. *Modern Pathology*, 22(4):489, 2009.

[22] Emmanuel Akintoye, Nitin Kumar, Hiroyuki Aihara, Hala Nas, and Christopher C Thompson. Colorectal endoscopic submucosal dissection: a systematic review and meta-analysis. *Endoscopy international open*, 4(10):E1030–E1044, 2016.

[23] Alberto Arezzo, Roberto Passera, Yutaka Saito, Taku Sakamoto, Nozomu Kobayashi, Naoto Sakamoto, Naohisa Yoshida, Yuji Naito, Mitsuhiro Fujishiro, Keiko Niimi, et al. Systematic review and meta-analysis of endoscopic submucosal dissection versus transanal endoscopic microsurgery for large noninvasive rectal lesions. *Surgical endoscopy*, 28(2):427–438, 2014.

[24] Takuji Gotoda, Hironori Yamamoto, and Roy M Soetikno. Endoscopic submucosal dissection of early gastric cancer. *Journal of gastroenterology*, 41(10):929–942, 2006.

[25] Ichiro Oda. A minimally invasive treatment for early gi cancers. *Cleveland Clinic journal of medicine*, 84(9):707, 2017.

[26] Byung Gon Kim, Hyuk Soon Choi, Sei Hoon Park, Jun Ho Hong, Jung Min Lee, Seung Han Kim, Hoon Jai Chun, Daehie Hong, and Bora Keum. A pilot study of endoscopic submucosal dissection using an endoscopic assistive robot in a porcine stomach model. *Gut and liver*, 13(4):402, 2019.

[27] Philippa F Middleton, Leanne M Sutherland, and Guy J Maddern. Transanal endoscopic microsurgery: a systematic review. *Diseases of the colon & rectum*, 48(2):270–284, 2005.

[28] CR Praveen. Transanal endoscopic microsurgery: Where it stands as of today? *World*, 4(2):109–115, 2011.

[29] John E Speich and Jacob Rosen. Medical robotics. *Encyclopedia of biomaterials and biomedical engineering*, 983:993, 2004.

[30] Anthony R Lanfranco, Andres E Castellanos, Jaydev P Desai, and William C Meyers. Robotic surgery: a current perspective. *Annals of surgery*, 239(1):14, 2004.

[31] Russell H Taylor. A perspective on medical robotics. *Proceedings of the IEEE*, 94(9): 1652–1664, 2006.

[32] Thomas P Cundy, Kunal Shetty, James Clark, Tou Pin Chang, Kumuthan Sriskandarajah, Nicholas E Gattas, Azad Najmaldin, Guang-Zhong Yang, and Ara Darzi. The first decade of robotic surgery in children. *Journal of pediatric surgery*, 48(4):858–865, 2013.

[33] Jaydeep H Palep. Robotic assisted minimally invasive surgery. *Journal of Minimal Access Surgery*, 5(1):1, 2009.

[34] Zheng Li and Philip Wai-Yan Chiu. Robotic endoscopy. *Visceral medicine*, 34(1): 45–51, 2018.

[35] DTH Moura, Hiroyuki Aihara, and Christopher C Thompson. Robotic-assisted surgical endoscopy: a new era for endoluminal therapies. *VideoGIE: an official video journal of the American Society for Gastrointestinal Endoscopy*, 4(9):399–402, 2019.

[36] Baldwin Po Man Yeung and Philip Wai Yan Chiu. Application of robotics in gastrointestinal endoscopy: A review. *World journal of gastroenterology*, 22(5):1811, 2016.

[37] M Brancadoro, C Quaglia, H Abidi, MA Bonino, A Arezzo, and A Menciassi. Surgical robotic platform for endoscopic dissection.

[38] Hyoung-Ki Lee and Myung Jin Chung. Adaptive controller of a master–slave system for transparent teleoperation. *Journal of Robotic systems*, 15(8):465–475, 1998.

[39] Alejandro Jarillo Silva, Omar A Domínguez Ramirez, Vicente Parra Vega, and Jesus P Ordaz Oliver. Phantom omni haptic device: Kinematic and manipulability. In *2009 Electronics, Robotics and Automotive Mechanics Conference (CERMA)*, pages 193–198. IEEE, 2009.

[40] Andreas Nygaard. High-level control system for remote controlled surgical robots: Haptic guidance of surgical robot. Master's thesis, Institutt for teknisk kybernetikk, 2008.

[41] Wayne John Book and Dirk Hannema. Master-slave manipulator performance for various dynamic characteristics and positioning task parameters. 1980.

[42] Padmaraja Yedamale. Brushless dc (bldc) motor fundamentals. *Microchip Technology Inc*, 20:3–15, 2003.

[43] Graham Clifford Goodwin, Stefan F Graebe, Mario E Salgado, et al. *Control system design*, volume 240. Prentice Hall New Jersey, 2001.

[44] Kiam Heong Ang, Gregory Chong, and Yun Li. Pid control system analysis, design, and technology. *IEEE transactions on control systems technology*, 13(4):559–576, 2005.

[45] Chul-Hwan Jung, Chang-Shik Ham, and Kuhn-Il Lee. A real-time self-tuning fuzzy controller through scaling factor adjustment for the steam generator of npp. *Fuzzy sets and systems*, 74(1):53–60, 1995.

[46] MF Rahmat. Application of selftuning fuzzy pid controller on industrial hydraulic actuator using system identification approach. In *International Journal on Smart Sensing and Intelligent Systems*. Citeseer, 2009.

[47] Khouloud Bedoud, Mahieddine Ali-rachedi, Tahar Bahi, and Rabah Lakel. Adaptive fuzzy gain scheduling of pi controller for control of the wind energy conversion systems. *Energy Procedia*, 74:211–225, 2015.

[48] Ge Yang and Tao Yang. A study of computational verb pid controllers: Structures and designs. *International Journal of Computational Cognition*, 7(3):61–73, 2009.

[49] Ralph Wittmann and Martina Zitterbart. *Multicast communication: Protocols, programming, & applications*. Elsevier, 2000.

[50] Keith Pazul. Controller area network (can) basics. *Microchip Technology Inc*, 1, 1999.

[51] Gianluca Cena and Adriano Valenzano. A protocol for automatic node discovery in canopen networks. *IEEE Transactions on Industrial Electronics*, 50(3):419–430, 2003.

[52] Reiner Zitzmann and Thilo Schumann. Interoperable medical devices due to standardized canopen interfaces. In *2007 Joint Workshop on High Confidence Medical Devices, Software, and Systems and Medical Device Plug-and-Play Interoperability (HCMDSS-MDPnP 2007)*, pages 97–103. IEEE, 2007.

[53] Charles E Spurgeon. *Ethernet: the definitive guide*. " O'Reilly Media, Inc.", 2000.

[54] Timo Kiravuo, Mikko Sarela, and Jukka Manner. A survey of ethernet lan security. *IEEE Communications Surveys & Tutorials*, 15(3):1477–1491, 2013.

[55] Paul Brooks. Ethernet/ip-industrial protocol. In *ETFA 2001. 8th International Conference on Emerging Technologies and Factory Automation. Proceedings (Cat. No. 01TH8597)*, volume 2, pages 505–514. IEEE, 2001.

[56] S Vijayachitra. *Communication Engineering*. Tata McGraw-Hill Education, 2013.

Phantom DLL

Listing 1 Phantom DLL Header

```
// Phantom_dll.h

/*#ifdef PHANTOM_DLL_EXPORTS
#define PHANATOM_DLL_API __declspec(dllexport)
#else
#define PHANATOM_DLL_API __declspec(dllimport)
#endif
*/
#include "stdafx.h"

typedef struct
{
  hduVector3Dd anchor;
  hduVector3Dd A;
  hduVector3Dd C;
  hduVector3Dd E;
  hduVector3Dd force;
  HDboolean bRenderForce;
  HDdouble gSpringStiffness;
} AnchorData;

// returns int referred to error
extern "C"
{
 __declspec(dllexport) int query_forcesHD(unsigned int* hHD, int*
    Button1, int* Button2, double pos[3], double ang[3], double
    anchor[3], double force[3], double A[3], double C[3], double E
    [3], int* bRenderForce, double* gSpringStiffness);
```

```
}

HDCallbackCode HDCALLBACK ForcesCallback(void* pUserData);
```

Listing 2 Phantom DLL Functions

```
/* Phantom_dll.cpp : Defines the exported functions for the DLL
application.*/

#ifdef  _WIN64
#pragma warning (disable:4996)
#endif

#include "stdafx.h"
#include "Phantom_dll.h"
#include <math.h>

using namespace std;

typedef struct
{
  HDint button1;         /*Device button #1 has been pressed*/
  HDint button2;         /*Device button #2 has been pressed*/
  HDboolean inkwell;
  hduVector3Dd pos;      /* Current device coordinates. */
  hduVector3Dd ang;      /* Current device orientation */
  hduVector3Dd joint;    /* Current device orientation */

  HDErrorInfo error;
} DeviceData;

extern "C"
{

/*******************************************************
Checks the state of the gimbal button and gets the angles
of the device. Useful for forward kinematics
*******************************************************/
  __declspec(dllexport) int query_forcesHD(unsigned int* hHD, int*
    Button1, int* Button2, double pos[3], double ang[3], double
   anchor[3], double force[3], double A[3], double C[3], double E
   [3], int* bRenderForce, double* gSpringStiffness) {
```

```
hdMakeCurrentDevice(*hHD);
DeviceData currentData;
AnchorData anchorPoint;
anchorPoint.anchor[0] = anchor[0];
anchorPoint.anchor[1] = anchor[1];
anchorPoint.anchor[2] = anchor[2];
anchorPoint.force[0] = force[0];
anchorPoint.force[1] = force[1];
anchorPoint.force[2] = force[2];
anchorPoint.A[0] = A[0];
anchorPoint.A[1] = A[1];
anchorPoint.A[2] = A[2];
anchorPoint.C[0] = C[0];
anchorPoint.C[1] = C[1];
anchorPoint.C[2] = C[2];
anchorPoint.E[0] = E[0];
anchorPoint.E[1] = E[1];
anchorPoint.E[2] = E[2];
anchorPoint.bRenderForce = *bRenderForce;
anchorPoint.gSpringStiffness = *gSpringStiffness;

HDdouble gMaxStiffness = 1.0;
HDErrorInfo m_error;

/* Performs a synchronous call to copy the most current
device state. This synchronous scheduler call
ensures that the device state is obtained in a
thread-safe manner. */
hdScheduleSynchronous(DeviceDataCallback, &currentData,
HD_DEFAULT_SCHEDULER_PRIORITY);

hdScheduleSynchronous(ForcesCallback, &anchorPoint,
HD_DEFAULT_SCHEDULER_PRIORITY);

*Button1 = currentData.button1;
*Button2 = currentData.button2;
pos[0] = currentData.pos[0];
pos[1] = currentData.pos[1];
pos[2] = currentData.pos[2];
ang[0] = currentData.ang[0];
ang[1] = currentData.ang[1];
ang[2] = currentData.ang[2];

/* Also check the error state of HDAPI. */
```

```
    m_error = hdGetError();

    /* Copy the position into our device_data structure. */
    force[0] = anchorPoint.force[0];
    force[1] = anchorPoint.force[1];
    force[2] = anchorPoint.force[2];

    return m_error.errorCode;
    }
}
/* Begin Callbacks*/

/******************************************************************
* Main scheduler callback for rendering forces.
******************************************************************/

HDCallbackCode HDCALLBACK ForcesCallback(void* pUserData)
{
  hduVector3Dd position;
  AnchorData* anchorPoint = (AnchorData*)pUserData;
  AnchorData actualAnchor;

  const HDdouble kForceInfluence = 10; /* mm */
  HDdouble difference[3];
  HDdouble vectorforce[3];
  HDdouble D[3];
  HDdouble O[3];
  HDdouble P[3];
  HDdouble gD[3];

  memcpy(&actualAnchor, anchorPoint, sizeof(AnchorData));
  actualAnchor.force.set(0, 0, 0);

  HDErrorInfo error;

  if (!hdIsEnabled(HD_FORCE_OUTPUT))
   hdEnable(HD_FORCE_OUTPUT);

  hdBeginFrame(hdGetCurrentDevice());
  hdGetDoublev(HD_CURRENT_POSITION, position);

  /* Compute spring force as F = k * (anchor - pos), which
  will attract the device position towards the anchor
  position if Sprin positive and will create a continuous
```

```
    force towards the anchor. If negative Spring, it will
    create a continuos force that pushes away*/
    if (anchorPoint->bRenderForce == 1) {
     hduVecSubtract(difference, actualAnchor.anchor, position);
     hduVecScale(actualAnchor.force, difference, actualAnchor.
     gSpringStiffness);
}
    /* Does the same thing as the previous case but renders the
    force only in a specific range around the point
    (kForceInfluence)*/
    else if (anchorPoint->bRenderForce == 2) {
     hduVecSubtract(difference, actualAnchor.anchor, position);

     if (hduVecMagnitude(difference) < kForceInfluence)
     {
      hduVecScale(actualAnchor.force, difference, actualAnchor.
     gSpringStiffness);
     }
    }
    /* Creates a force along a line: needs two points defined:
    A and C */
    else if (anchorPoint->bRenderForce == 3) {
    /* P is the point in line AC which will be useful to
    create the vector normal to line AC that passes B, B
    is the current position of the phantom. The variable
    v is unknown and gives the magnitude of the vector
    that goes from A to P.
    (1) P = A + v(C-A)
    (2) (B-P)dotproduct(C-A) */

    // C-A
    hduVecSubtract(D, anchorPoint->C, anchorPoint->A);
    // B-A
    hduVecSubtract(O, position, anchorPoint->A);

    HDdouble OD = hduVecDotProduct(O, D);
    HDdouble D2 = hduVecDotProduct(D, D);
    HDdouble g = OD / D2;

    hduVecScale(gD, D, g);
    hduVecAdd(P, anchorPoint->A, gD);

    hduVecSubtract(vectorforce, P, position);
    if (actualAnchor.gSpringStiffness < 0) {
```

```
    if (hduVecMagnitude(vectorforce) < kForceInfluence)
    {
     hduVecScale(actualAnchor.force, vectorforce, actualAnchor.
    gSpringStiffness);
    }
   }
   else if (actualAnchor.gSpringStiffness > 0) {
    hduVecScale(actualAnchor.force, vectorforce, actualAnchor.
    gSpringStiffness);
   }
  }
   /* Creates a forces along plane, constrains the movement
   along this plane if Spring negative. To define a plane
   we need three points A,C and E. The vectors   CA and EA
   are used to compute the cross product to find the normal
   vector to the plane, then this        vector is used to find
   the vector perpendicular to the plane that passes
   through point B (current position).
   CA = A-C
   EA = A-E
   n = CAxEA      */
   else if (anchorPoint->bRenderForce == 4) {
    HDdouble CA[3];
    HDdouble EA[3];
    HDdouble n[3];
    HDdouble F;
    HDdouble res[3];
    HDdouble vd[3];
    HDdouble dev;
    HDdouble mag;
    HDdouble norm[3];

    hduVecSubtract(CA, anchorPoint->A, anchorPoint->C);
    hduVecSubtract(EA, anchorPoint->A, anchorPoint->E);

    hduVecCrossProduct(n, CA, EA);
    F = -(n[0]*CA[0] + n[1]*CA[1] + n[2]*CA[2]);
    mag = hduVecMagnitude(n);
    hduVecNormalize(norm, n);
    dev = (n[0]*position[0] + n[1]*position[1] + n[2]*position[2] +
     F)/mag;
    hduVecScale(res, norm, dev);
```

```
    hduVecScale(actualAnchor.force, res, actualAnchor.
    gSpringStiffness);
  }

  hdSetDoublev(HD_CURRENT_FORCE, actualAnchor.force);
  hdEndFrame(hdGetCurrentDevice());

  memcpy(anchorPoint, &actualAnchor, sizeof(AnchorData));

  /* Check if an error occurred while attempting to render
  the force */
  if (HD_DEVICE_ERROR(error = hdGetError()))
  {
   if (hduIsForceError(&error))
   {
    hdDisable(HD_FORCE_OUTPUT);
   }
   else if (hduIsSchedulerError(&error))
   {
    return HD_CALLBACK_DONE;
   }
  }
  return HD_CALLBACK_DONE;
}
```